AN ELECTRICAL ANALOG FOR INVESTIGATING INCOMPRESSIBLE FLUID FLOW WITH LOSSES

William Chi-Ting Chu

A DISSERTATION

in

The Faculty

of

Engineering

Presented in Partial Fulfillment of the Requirements for
the Degree of Master of Engineering at
Sir George Williams University
Montreal, Canada

September, 1972

AN ELECTRICAL ANALOG FOR INVESTIGATING INCOMPRESSIBLE FLUID FLOW WITH LOSSES

by

William Chi-Ting Chu

ABSTRACT

An electrical analog using field plot for investigating the velocity and pressure distributions of incompressible flows in pipes with variable cross-sectional area was developed. The electrical potential measured in the electrical model is analogous to the total energy of the fluid flowing through the prototype. The equipotential surface of the electrical model is analogous to the equipotential surface of the flow field in the prototype, which is perpendicular to the streamlines of the flow. On the equipotential surface of the flow, the pressure and velocity are respectively constant, and can be determined by using the continuity condition. The basic assumption of the analysis is that the total loss across the flow system is known.

Applications of the electrical analog to flows through tubes with different enlargements were made. The results obtained from the electrical analog are in good agreement with that obtained by the experiments with pitot tube measurements.

ACKNOWLEDGEMENTS

The author wishes to express his gratitude and appreciation to his supervisor, Dr. S. Lin for providing his encouragement and valuable advice throughout the experimental study.

The author also wishes to thank all individuals for their assistance in experimental preparation, typing, drafting and correction of proofs of the manuscript.

This work was supported by the National Research Council of Canada (NRC) under Grant No. A-7929.

TABLE OF CONTENTS

PAGE

LIST OF FIGURES

NOTATIONS

A, A_1, A_2	area, and areas before and after the expansion, respectively
a, a_s	acceleration, and acceleration along s-direction, respectively
D, D_1, D_2	diameter, and diameters before and after the expansion of the circular pipe, respectively
E. P.	electric plottings
e, e	electric voltage; roughness of fluid flowing pipe
f	friction factor of the fluid flowing through the axisymmetric duct
f_a	electric/fluid analog proportionality
f_s	similitude proportionality of model/prototype
h	head loss
L, ℓ	length of fluid flowing along axial direction
M, m	mass, and mass per unit, respectively
$\dot{M}$, $\dot{m}$	mass flowrate and flowrate per unit mass, respectively
P, P_1, P_2	pressure, and pressures before and after the expansion, respectively
P.M.	measurements, pitot tube
Q	volume flow rate
R_c	Reynold's number
u, v, w	velocity component along x, y and z-direction, respectively
V, V_1, V_2	velocity, and velocities before and after the expansion of the fluid flow, respectively
$\bar{V}$	dimensionless factor = $\dfrac{V}{\sqrt{2g\Delta h_{1,2}}}$
V^2	velocity in combination with two-dimensional flow = $u^2 + w^2$

α	fractional number, dimensionless
α_c	correction value of α
α_m, α_p	fractional number of potential voltage in model, and total head loss in prototype, respectively
β	half graduate angle of an enlargement
β_c	replacement of β for the evaluation of the experimental results
$\Delta h_{1\cdot 2}$	magnitude of the change of head loss in fluid flow pipe within the regions of 1 and 2.
ΔP	dimensionless factor $= \frac{P_1 - P}{\rho g \Delta h_{12}}$
ξ	vorticity $= [\frac{\partial w}{\partial x} - \frac{\partial u}{\partial z}]$ in two-dimensional flow
ρ	density of flowing fluid
ρ_x	resistivity along x-axis direction
X	the distances along x-axis direction

CHAPTER I

INTRODUCTION

CHAPTER I

INTRODUCTION

An analog is often used to explain an unfamiliar or difficult matter, concept, or idea, in terms of a better-known or a simpler case. In this experimental study, the electric analog makes use of the fact that a flow of an electric current through a thin, uniform conducting paper produces an electric potential voltage distribution within a region on the boundary, on which the analog is being based. The correspondence between the voltage in the conducting paper and the distribution of potential energy in the fields of the fluid flowing duct, may bear an analog to one another.

Many engineering problems are solved by using the knowledge of potential-field distributions involved. Such problems may be concerned with mechanics, heat transfer, streamlined fluid flow, etc. Some of the problems may be solved mathematically by finding solutions to the equations. However, when the boundary conditions become complicated, a mathematical solution is very tedious. [1,2]

Applications of electric analog may be illustrated in various fields of mechanical engineering. [3,4,5,6] For

instance, the vibration of a weight suspended from a spring has been investigated by studying the analog system of an inductance-capacitance circuit, as shown in Fig. 1. In this case, the equation for the mechanical system can be expressed as

$$F = M\frac{d^2x}{dt^2} + k\frac{dx}{dt} + Sx$$

or

$$F = M\frac{dv}{dt} + k\,v + S\int v\,dt \qquad (1.1)$$

and the equation for the electrical system

$$E = L\frac{di}{dt} + R\,i + \frac{1}{C}\int i\,dt \qquad (1.2)$$

where the f, M, k and S indicate the force, mass, friction, and stiffness in the mechanical system; and E, L, R and C denote the e.m.f., inductance, resistance, capacitance in the electrical system, respectively.

By using an analogy, we may say that

$$\text{In mechanical system} \left\{ \begin{array}{rcl} F & \simeq & E \\ M & \simeq & L \\ k & \simeq & R \\ S & \simeq & \frac{1}{C} \end{array} \right\} \text{In electrical system}$$

In practice, it is much easier to investigate the electrical system, e.g., it is much simpler to use an adjustable capacitor than to make a spring of adjustable stiffness.

As the equipment and the technology are being develop-

ed successively, the use of analog and the confidence in analog studies have steadily increased in various fields of application. The other justification for the use of the electric analog is to provide a rapid and inexpensive method of comparing the conventional experiment on the prototype.

The objectives of this experimental study may be categorized as follows:

1) With the selected equipment in order to perform the experiment, basically formulate the voltage analog to the relevance of energy in the fluid flow system as being considered by Kirshner.[7]

2) Experimentally solve the fluid equations of energy for investigating the incompressible flow with losses in an axisymmetric of variable cross-sectional ducts.

3) By the use of the experimental model test results combined with the suitable correction developed, a comparison with the conventional experiment [8] can be performed.

4) Accordingly, the pressure, velocity and losses of energy distributions along the axial direction of incompressible flow may be investigated and predetermined by using the corrected results obtained from the electric analog model experiment.

As the conservation equations for steady, incompressible flow in a variable cross-sectional duct, it will usually be necessary to use more complicated equipment or facilities to achieve this purpose. [9,10] The present analytical development and the experiment employed for investigating the pressure, velocity and losses of energy distributions in the flowing fluid are likely to be useful, greatly simplifying the applications in practical engineering performance.

CHAPTER II

BASIC ANALYSIS

CHAPTER II

BASIC ANALYSIS

Although certain general characteristics of fluid flow in streamline or in streamtube form can be interpreted through the use of the basic energy equations of motion, an expression of the phenomena in suitable mathematical form is still required for the present experimental study to be workable in approaching problems involving the energy distributions in an incompressible fluid flow with losses.

2.1 THE VOLTAGE ANALOG

Since the energy equation for fluid flowing through a streamtube concerns the state of energy flow, it is actually a power equation, as follows:

$$dP_m = \dot{m}\, d(P/\rho + V^2/2 + Zg) \qquad (2.1)$$

where

P_m = mechanical power
$\dot{m}$ = mass flow rate
P/ρ = pressure work
$V^2/2$ = kinetic work
Zg = potential work

For an electric system, the electric power lost through the resistance in an electric circuit is given by

$$dP_e = i\ de \tag{2.2}$$

where

P_e = electric power

i = electric current

e = voltage

From eqns. (2.1) and (2.2) the fluid/electric analog may be established as follows:

$$dP_e \simeq dP_m \tag{2.3}$$

$$i \simeq \dot{m} \tag{2.4}$$

$$de \simeq d(P/\rho + V^2/2 + Zg) \tag{2.5}$$

In a steady, incompressible, and isothermal fluid flow, where g and ρ both are constant, then the equivalent equation of analog (2.5) becomes

$$\begin{aligned} \Delta e &= e_1 - e_2 \\ &\simeq (P_1 - P_2)/\rho + \\ &+ (V^2{}_1 - V^2{}_2)/2 + (Z_1 - Z_2)g \end{aligned} \tag{2.6}$$

where subscripts 1 and 2 indicate the initial and final sections of the fluid flowing system, respectively.

2.2 THE RELEVANCE OF MATHEMATICAL FORMULATIONS FOR THE ELECTRICAL ANALOG EXPERIMENT

2.2.1 One-Dimensional Flow

As shown in Fig. 2, consider a streamline or stream-

tube of differential cross-section, the forces tending to accelerate the cylindrical fluid mass are : pressure forces on the ends of the element

$$P\,dA - (P + dP)dA = -\,dP\,dA \tag{2.7}$$

and the component of weight in the direction of motion

$$-\rho g ds\, dA(dz/ds) = -\rho g dA\, dz \tag{2.8}$$

The differential mass being accelerated by the action of these differential forces is

$$dM = \rho ds\, dA \tag{2.9}$$

Applying Newton's second law

$$dF = (dM)a \tag{2.10}$$

and using the one-dimensional expression for acceleration

$$a = \frac{d^2s}{dt^2} = \frac{d}{dt}\left(\frac{ds}{dt}\right) = \frac{dV}{dt} = \frac{dV}{ds}\frac{ds}{dt} = V\frac{dV}{ds} \tag{2.11}$$

Substituting eqns. (2.7),(2.8),(2.9) and (2.11) into (2.10)

$$-\,dP\,dA - \rho g dA\,dz = (\rho ds\,dA)\,V\frac{dV}{ds} \tag{2.12}$$

Dividing eqn. (2.12) by ρdA, the one-dimensional fluid flow equation becomes

$$\frac{dP}{\rho} + V\,dV + gdz = 0 \tag{2.13}$$

Eqn. (2.13) is familiar to us as Euler's equation, and dividing each term by g it becomes

$$\frac{dP}{\rho g} + d\left(\frac{V^2}{2g}\right) + dz = 0 \qquad (2.14)$$

For incompressible flow, the one-dimensional Euler's equation may be easily integrated (since ρ and g are both constant)

$$\int \frac{dP}{\rho g} + \int d\left(\frac{V^2}{2g}\right) + \int dz = \text{Constant}$$

to obtain Bernoulli's equation

$$\frac{P}{\rho g} + \frac{V^2}{2g} + z = h(\text{termed total head}) \qquad (2.15)$$

which will apply to all points on the streamline and thus provide a useful relationship between pressure P, velocity V and height above datum z.

Bernoulli's eqn. (2.15), may also be derived from energy considerations to shed more light on its significance and utility. As shown in Fig. 3, for one pound weight of fluid the kinetic energy may be written direction from considerations of mechanics: the general expression for kinetic energy of translation is $M V^2/2$; for unit weight of fluid, however, $M = 1/g$, so the kinetic energy becomes $V^2/2g$ (ft-lb)/lb. Similarly, the potential energy of a weight W at a vertical distance z above datum is Wz(ft-lb); or simply z(ft-lb)/lb for a unit weight of fluid.

Restricting the derivation to steady flow and considering the continuity principle, each unit weight of fluid

entering the boundary region within the sections through Section 1 must displace a unit weight of fluid which will move out of the boundary across Section 2. Therefore

$$\left[\begin{matrix}\text{Energy carried in by each unit weight of} \\ \text{fluid}\end{matrix}\right] = \frac{V^2_1}{2g} + z_1$$

$$\left[\begin{matrix}\text{Energy carried out by each unit weight of} \\ \text{fluid}\end{matrix}\right] = \frac{V^2_2}{2g} + z_2$$

Now consider the work done on fluid within the boundary by a weight of fluid entering the boundary, and that done by the fluid within the boundary on the same weight of fluid leaving. Suppose that in a certain time a weight of fluid $\rho g ds_1 dA_1$ moves into the boundary across Section 1 and that in this time, a weight of fluid $\rho g ds_2 dA_2$ leaves the boundary across Section 2. The work associated with these displacements can be computed from the products of the forces $P_1 dA_1$ and $P_2 dA_2$ and displacements ds_1 and ds_2 which give $P_1 dA_1 ds_1$ and $P_2 dA_2 ds_2$, respectively. For simplification and convenience, these work terms may be written per unit weight of fluid flowing; this can be done by dividing by the total weight of fluid ($\rho g ds_1 dA_1$ and $\rho g ds_2 dA_2$) doing the work; the results are $P_1/\rho g$ and $P_2/\rho g$, respectively. Thus the energy equation may be expressed

$$\begin{matrix}\text{Energy entering} \\ \text{boundary}\end{matrix} + \begin{matrix}\text{Net work done on fluid} \\ \text{within boundary}\end{matrix} = \begin{matrix}\text{Energy leav-} \\ \text{ing boundary}\end{matrix}$$

or

$$\left(\frac{V_1^2}{2g} + z_1\right) + \left(\frac{P_1}{\rho g} - \frac{P_2}{\rho g}\right) = \left(\frac{V_2^2}{2g} + z_2\right)$$

which when rearranged is recognized as Bernoulli's equation

$$P_1/\rho g + V_1^2/2g + z_1 = P_2/\rho g + V_2^2/2g + z_2 \qquad (2.16)$$

From the form of Bernoulli's equation, it is natural that the flow work terms $P/\rho g$ become associated with the energy terms, $V^2/2g$ and z.

2.2.2 Two-Dimensional Flow

For a vertical two-dimensional flowfield it may be derived by applying Newton's second law to Euler's equation. As shown in Fig. 4, a basic differential element of fluid of dimensions dx by dz, and the forces dF_x and dF_z in such an element may be identified by following equations

$$dF_x = \frac{P_A+P_D}{2}\,dz - \frac{P_B+P_C}{2}\,dz \qquad (2.17)$$

$$dF_z = \frac{P_A+P_B}{2}\,dx - \frac{P_C+P_D}{2}\,dx - dW \qquad (2.18)$$

where $P_A = P$, $P_B = P+\frac{\partial P}{\partial x}\,dx$ and $P_D = P+\frac{\partial P}{\partial z}\,dz$

$$P_C = P+\frac{\partial P}{\partial x}\,dx + \frac{\partial P}{\partial z}\,dz$$

Substituting into eqns. (2.17) and (2.18) with appropriate pressures they reduce to

$$dF_x = -\frac{\partial P}{\partial x}\,dx\,dz \qquad (2.19)$$

$$dF_z = -\frac{\partial P}{\partial z}\,dx\,dz - \rho g\,dx\,dz \qquad (2.20)$$

The accelerations of the element may be derived as

$$a_x = u\frac{\partial u}{\partial x} + w\frac{\partial u}{\partial z} \qquad (2.21)$$

$$a_z = u\frac{\partial w}{\partial x} + w\frac{\partial w}{\partial z} \qquad (2.22)$$

Applying Newton's second law by equating the differential forces to the products of the mass of the element and respective accelerations, in eqns. (2.19) and (2.22)

$$-\frac{\partial P}{\partial x}\,dx\,dz = \rho dx\,dz\left(u\frac{\partial u}{\partial x} + w\frac{\partial u}{\partial z}\right) \qquad (2.23)$$

$$-\frac{\partial P}{\partial z}\,dx\,dz - \rho g\,dx\,dz = \rho dx\,dz\left(u\frac{\partial w}{\partial x} + w\frac{\partial w}{\partial z}\right) \qquad (2.24)$$

which by cancellation of dx dz and rearrangement reduce to Euler's equations of two-dimensional flow in a vertical plane

$$-\frac{1}{\rho}\frac{\partial P}{\partial x} = u\frac{\partial u}{\partial x} + w\frac{\partial u}{\partial z} \qquad (2.25)$$

$$-\frac{1}{\rho}\frac{\partial P}{\partial z} = u\frac{\partial w}{\partial x} + w\frac{\partial w}{\partial z} + g \qquad (2.26)$$

Accompanied by the equation of continuity

$$\frac{\partial u}{\partial x} + \frac{\partial w}{\partial z} = 0 \qquad (2.27)$$

Euler's equations form a set of three simultaneous partial differential equations which are basic to the solution of a

two-dimensional flowfield; a complete solution of these equations will yield P, u, and w as the functions of x and z, allowing the prediction of pressure and velocity at any point in the flowfield.

Bernoulli's equation may be derived by integrating Euler's equations, as was done for the one-dimensional flow, as follows: Multiplying (2.25) by dx and (2.26) by dz and adding them

$$-\frac{1}{\rho}\left(\frac{\partial P}{\partial x}\,dx+\frac{\partial P}{\partial z}\,dz\right) = u\frac{\partial u}{\partial x}\,dx + w\frac{\partial u}{\partial z}\,dx +$$

$$+ u\frac{\partial w}{\partial x}\,dz + w\frac{\partial w}{\partial z}\,dz + g\,dz$$

The terms $w(\partial w/\partial x)dx$ and $u(\partial u/\partial z)dz$ are added to and subtracted from the right-hand side of the equation, and the terms then collected in the following pattern

$$-\frac{1}{\rho}\left(\frac{\partial P}{\partial x}dx+\frac{\partial P}{\partial z}dz\right) = \left(u\frac{\partial u}{\partial x}dx+w\frac{\partial w}{\partial x}dx\right) + \left(u\frac{\partial u}{\partial z}dz+w\frac{\partial w}{\partial z}dz\right)$$

$$+ (udz-wdx)\left(\frac{\partial w}{\partial x}-\frac{\partial u}{\partial z}\right) + g\,dz$$

The bracket on the left-hand side of this equation will be recognized as the total differential dP. The sum of the first two brackets on the right-hand side is easily shown to be $d(u^2+w^2)/2$, and the third bracket is identified as the vorticity, ξ. [16] Reducing the equation accordingly and dividing it by g, it may be written as

$$-\frac{dP}{\rho g} = \frac{d(u^2+w^2)}{2g} + \frac{1}{g}(udz-wdx)\xi + dz$$

and integrated to

$$\frac{P}{\rho g} + \frac{u^2+w^2}{2g} + z = h - \frac{1}{g}\int(udz-wdx)\xi$$

in which h is the constant of integration. Since the resultant velocity V at any point in the flowfield is related to its components u and w by $V^2 = u^2 + w^2$, the equation further simplifies to

$$\frac{P}{\rho g} + \frac{V^2}{2g} + z = h - \frac{1}{g}\int\xi(udz-wdx) \qquad (2.28)$$

This equation thus shows that the sum of Bernoulli terms at any point in a flowfield will be a constant h if the vorticity ξ is zero, i.e., if the flowfield is an irrotational one. Thus for irrotational flow, the same constant applies to all the streamlines of the flowfield, or, in terms of the energy line the Bernoulli equation may be applied over the flowfield of an ideal incompressible fluid with a single energy line completely describing the energy situation. In Fig. 5, this may be shown as two representative points A and B. From the position of the points (above datum) the quantity $(P/\rho g + \frac{V^2}{2g})$ may be determined from the position of the energy line, but the pressures P_A, P_B, etc., cannot be calculated until the corresponding velocities V_A, V_B, are known. [1,8,16]

2.2.3 Applying Bernoulli's Equation of Energy Line to the Electric Analog Model Experiment

For an irrotational incompressible flow of real fluid with energy dissipation Bernoulli's eqn.(2.28) and the analog eqn. (2.6), may be written

$$P_1/\rho g+V_1^2/2g + z_1 = P_2/ g+V_2^2/2g + z_2 + \Delta h_{1.2}$$

or

$$(P_1-P_2)/\rho g + (V_1^2-V_2^2)/2g + (z_1-z_2) = \Delta h_{1.2} \quad (2.29)$$

where Δh_{12} is frequently termed as head loss through the total region of fluid flowing from Section 1 to Section 2. As shown in experiments on the fluid flowing in long straight, cylindrical ducts the value of Δh_{12} is varied directly with velocity head, $V^2/2g$ and the duct length ℓ , and inversely with duct diameter, D. Using proportionality f, D'Arcy, Weishach and Fanning [16] proposed equations of the same form, independently

$$\Delta h_{12} = f \frac{\ell}{D} \frac{V^2}{2g} \quad (2.30)$$

where f is usually called friction factor of dimensionless.

Thus for real fluid flow, with eqn. (2.29) eqn. (2.6) may reduce to

$$\begin{aligned} \Delta e &= e_1-e_2 \\ &\simeq (P/\rho+V^2/2+zg)_1 - (P/\rho+V^2/2 + zg)_2 \quad (2.31) \\ &= g\Delta h_{1.2} \end{aligned}$$

Alternatively, eqns. (2.29) and (2.31) may be

depicted by graphically sketching, as shown in Fig. 6. For the position of the points within the region between Sections 1 and 2, the velocity and pressure that are desired in the flowfield and under the incompressible and steady stream of real fluid flow conditions, may be described by eqn.(2.31) combined with the equation of continuity

$$\rho_1 A_1 V_1 = \rho_2 A_2 V_2 = \rho A\, V$$

and for incompressible fluid flow throughout the system

$$\rho_1 = \rho_2 = \rho$$

Thus eqn. (2.31) may reduce to

$$(P_1-P)/\rho + (V_1^2-V^2)/2 + (z_1-z)g = \alpha_p g\Delta h_{1\cdot 2} \qquad (2.32)$$

and the corresponding electrical analog equation will be

$$e_1-e = \alpha_m \Delta e_{1\cdot 2} \qquad (2.33)$$

where α_p and α_m are both fractional numbers of dimensionless of fluid flow prototypes and of electric analog models, respectively. Dividing each term of eqn. (2.32) by $g\Delta h_{1\cdot 2}$, we have

$$(P_1-P)/\rho g\Delta h_{1.2} + (V_1^2-V^2)/2g\Delta h_{1.2} + (z_1-z)/\Delta h_{1.2} = \\ = \alpha_p \qquad (2.34)$$

From the equation of continuity and for an incompressible fluid flow being assumed, eqn. (2.34) can be reduced to

$$(P_1-P)/\rho g\Delta h_{1.2} + \frac{V_1^2}{2g\Delta h_{1.2}}\left[1 - \left(\frac{A_1}{A}\right)^2\right] + (z_1-z)/\Delta h_{1.2} = \\ = \alpha_p \qquad (2.35)$$

with simplifying, rewrite eqn. (2.35) as

$$\Delta P + \bar{V}_1^2\left[1 - \left(\frac{A_1}{A}\right)^2\right] + (z_1-z)/\Delta h_{1.2} = \\ = \alpha_p \qquad (2.36)$$

where

$$\Delta P = (P_1-P)/(\rho g\Delta h_{1.2}) \qquad (2.37)$$

$$\bar{V}_1 = V_1/(2g\Delta h_{1.2})^{\frac{1}{2}} \qquad (2.38)$$

In horizontal duct flow, and as in many cases of engineering applications the potential term (z_1-z) may be negiligible, thus eqn. (2.36) becomes

$$\Delta P + \bar{V}_1^2\left[1 - \left(\frac{A_1}{A}\right)^2\right] = \alpha_p \qquad (2.39)$$

For solving eqn. (2.39) experimentally a proportionality factor, f_a, of the fluid/electric analog has to be introduced.

Now from eqn. (2.32), with neglecting the change of

elevation, and eqn. (2.33), we define

$$f_a = \frac{e_1 - e}{\Delta P - \bar{V}_1^2[1 - (\frac{A_1}{A})^2]} = \frac{\alpha_m \Delta e_{1.2}}{\alpha_p g \Delta h_{1.2}}$$

which is in units of $(\text{volt})(\text{sec.})^2(\text{ft})^{-2}$, and set $\alpha_m = \alpha_p$, since both of them are numerical values of dimensionless, then

$$f_a = \frac{\Delta e_{1.2}}{g \Delta h_{1.2}} \tag{2.40}$$

In the experimental study of the electric model the value of α_m, along the axial direction, can be determined, and that of (A_1/A) can then be located accordingly. With a knowledge of the values of α_p, and (A_1/A), eqn. (2.39) may then be solved for giving the initial fluid flow conditions.

CHAPTER III

EXPERIMENTAL EQUIPMENT AND PROCEDURE

CHAPTER III

EXPERIMENTAL EQUIPMENT AND PROCEDURE

The experimental performance is based on the foregoing basic analysis of equations developed.

3.1 EXPERIMENTAL EQUIPMENT

The main equipment used in the experimental study of the electric analog consists of a field plotter, as shown in Fig. 7, which is developed by Servomex Controls Limited. The plotter consists of a stabilized A.C. supply of 100-250 voltage, fed to a wire potentiometer which provides a convenient source for obtaining boundary voltage values for the conducting paper specimen. A 4-7 kilo-ohms and a 10 kilo-ohms potentiometer are used for the adjustment purposes. Flexible leads are used for selecting the boundary voltage values from the wire potentiometer, connections being made to the wire by spring loaded clips. Voltages, as selected points of the specimen, are determined by balancing the probe voltage at the selected point by a corresponding voltage tapped from the wire potentiometer. An oscilloscope is used as a null indicator, and the balancing voltage is measured by means of an Avometer. The electric circuit diagram is shown in Fig. 8.

The conducting paper, which is used as a conduit for flow of current, is a thin, uniform resistance sheet. It is obtainable commercially as Teledeltos paper. By means

of a special probe connected to the field plotter one can measure the voltage at any point on the paper, and thus prepare a set of equipotential lines of flowing along the axial direction.

There may be some variable resistivities measured along the roll and across the roll of the resistance paper. These defects can be corrected, if it is necessary, by modifying the specimen dimensions with multiplying measurements taken across the paper : · the factor (ρ_y/ρ_x), where ρ_x is the resistivity along the ·ll and ρ_y is the resistivity across the roll.[4] The tailed derivation of the correction factor is as shown in A. ndix I.

As the results shown in Figs. 9 and 10, the strip a b c d is cutting across the roll and the strip a'b'c'd' cuts along the roll. The length of a b is equal to that of a'b', and the dimensions of the two strips are both 2 in.by 6 in. After plotting,the potential differences between the two strips, as shown in Fig. 10 seem to be negligible. Thus, there is no such correction required in later proceedings presented.

Another material accompanied in the experimental proceedings is the conducting paint, which is a dispersion of silver in methyl-butyl-ketone

$$\left(CH_3 - \overset{CH_3}{\overset{|}{C}}\overset{H}{\overset{|}{-}}\overset{H}{C} - C - CH_3 \right)$$

Although the paint bottle seals are effective, it is advisable to keep the bottle as cool as possible, especially in hot climates. The paint is easily applied on the resistance paper to stick the electrodes together.

3.2 EXPERIMENTAL PROCEDURE

The following steps should be taken in preparing and performing an experiment to obtain a model field plotting. For simplifications, it is assumed that the dimensions of the electric model are identical with that of the prototype.

For the experiment the configurational dimensions of the selected mode, as shown in Fig. 11, are

A_1 = the cross-section of the inlet
= 1 in^2

A_2 = the cross-section of the outlet
= 3 in^2

$X_1 = X_2$

After choosing the configuration of the electric model it is necessary to fix the resistance paper of the model selected onto a suitable board with transparent adhesive tape, the pale grey side being uppermost. The electrodes are then painted on. The paint must be well stirred before application. The width of the electrodes need not exceed 1 cm and in many cases, may be only 0.2 cm. Connections to the

electrodes may be made by holding the wire to the paper with transparent adhesive tape and painting in the connecting wire to the electrode. An electrode must be at the same potential throughout and suitable additional connections must be made, if necessary.

As a suitable drying time has elapsed (usually about ten to fifteen minutes) the plotting can then proceed. The connecting wires are led to the field plotter terminals. With the potentiometer set to 0% and 100%, in turn, the appropriate electrodes must be tested to ensure that they are at the same potential throughout. The calibrated potentiometer is then set at an intermediate value. Proceed the plottings on the model as in Fig. 11, and get the results of equipotential lines, as shown in Fig. 12.

The number of equipotential lines, as shown in Fig. 12,is based upon both at intervals of 10% of the total voltage drop between the electrodes and in the regions of interest. Once the number of equipotential lines are plotted,a series of numerical values of α_m are determined and the graphical measurements of the cross-sectional area $(A)_m$ can be obtained directly over the entire flowing path along the axial direction.

In the electric analog model plottings, as shown in Fig. 12, the results of α_m plotted and the corresponding of $(A_1/A)_m$ located, are both in numerical values of dimensionless; thus the respective values of α_p and

$(A_1/A)_p$, should be the same magnitude in all sections accordingly in the similitude prototype of fluid flowing system.

Along the axial direction, the center-line values of velocity and pressure distributions that are evaluated from the analog model plottings should be the same as that in the similitude prototype of the fluid flowing system, as demonstratively shown in Fig. 13. The detailed calculation is as shown in Appendix 2.

CHAPTER IV

COMPARISON AND DISCUSSION OF THE RESULTS OBTAINED WITH THAT BEING PERFORMED BY OTHER EXPERIMENTAL DATA

CHAPTER IV

COMPARISON AND DISCUSSION OF THE RESULTS OBTAINED WITH THAT BEING PERFORMED BY OTHER EXPERIMENTAL DATA

The fluid flowing prototype of enlargement, of which the fluid flow characteristics has been measured experimentally by Chaturvedi [8] with stagnation tube and pitot tube, is being selected for the comparison. The dimensions of the prototype, as shown in Fig. 14, are: $D_1 = 4.25$ in., $D_2 = 8.50$ in., the fluid flowing length, $L = 104$ in., and the magnitude of the Reynold's number, R_e, is adjusted at about 2×10^5 at the intake of Section 1. The flowing fluid is of air and an incompressible flow is assumed by Chaturvedi during the measurements of velocity and pressure along the axial direction with the stagnation tube and pitot tube.

Without loss of generality, the prototype with the half graduate angles, β, of 15° and 90°, is being plotted in the corresponding analog electric model. The results, in addition to the suitable correction performance, obtained by the electric analog model plottings, are being compared with that performed experimentally by Chaturvedi in his measurements. [8]

For a comparison of the results, the following step-by-step procedure is conducted in accordance with the given prototype, and based on the basic analysis developed in the experimental study.

4.1 TRANSFORMING THE DIMENSIONS CITED IN FLUID PROTOTYPE TO THAT IN RESPECTIVE ANALOG MODEL FOR ELECTRICAL PLOTTINGS

The transformation is based on the fact that any equipotential curve plotted in the electric model represents an area perpendicular to the fluid flow in the prototype. As shown in Fig. 14, for similarity and analog modelling, the dimensions will be transformed as follows

(a) $\beta = 90^{o}$

In the prototype	In the model
$(A_1)_p = \frac{\pi}{4}(D_1)_p^2$	Set $(A_1)_m = 0.5\ in^2 = f_s^2 \frac{\pi}{4}(D_1)_p^2$
	$= f_s^2 (A_1)_p$
$(A_2)_p = \frac{\pi}{4}(D_2)_p^2$	$(A_2)_m = f_s^2 (A_2)_p = \frac{0.5}{\frac{\pi}{4}(D_1)_p^2} \cdot \frac{\pi}{4}(D_2)_p^2$
	$= 0.5(D/D_1)^2$
$(X/D_1)_p$	$(A_x/A_1)_m = \frac{\frac{\pi}{4} f_s^2 (X)_p^2}{\frac{\pi}{4} f_s^2 (D_1)_p^2}$
	$= (X/D_1)_p^2$

where we set $(A_1)_m = 0.5\ in^2$ in reference to the prototype configuration to make the experimental model workable, and f_s^2 is defined as

$$f_s^2 = \frac{(A_1)_m}{(A_1)_p} = \frac{0.5}{\frac{\pi}{4}(D_1)_p^2}$$

(b) $\beta = 15^o$

For the purpose of transforming the graduate portion in the prototype to that in the model accordingly the following procedure has to be undertaken, as shown in Fig. 15 (a), and Fig. 15 (b), respectively.

In the prototype, as shown in Fig. 15 (a), since $\tan \beta = \tan 15^o = 0.268$, then the length of the graduate portion becomes

$$(X_2)_p = \frac{(D_2-D_1)/2}{\tan 15^o} = 7.90 \text{ in.}$$

Dividing $(X_2)_p$ into five parts equally, thus, we have

$$(X_1)_{p_1} = \frac{(X_2)_p}{5} = 1.58 \text{ in}$$

$$(X_1)_{p_1} = \frac{2(X_2)_p}{5} = 3.16 \text{ in}$$

$$(X_1)_{p_3} = \frac{3(X_2)_p}{5} = 4.74 \text{ in}$$

$$(X_1)_{p_4} = \frac{4(X_2)_p}{5} = 6.32 \text{ in}$$

and the values of $(D_1)_{p_1}$ to $(D_2)_p$ can be calculated by

$$\tan 15^o = 0.268 = \frac{[(D_1)_{p_1} - (D_1)_p]/2}{(X_1)_{p_1}}$$

Then

$$(D_1)_{p_1} = 2(X_1)_{p_1}(0.268)+(D_1)_p = 5.10 \text{ in}$$

$$(D_1)_{p_2} = 2(X_1)_{p_2}(0.268)+(D_1)_p = 5.92 \text{ in}$$

$$(D_1)_{p_3} = 2(X_1)_{p_3}(0.268)+(D_1)_p = 6.80 \text{ in}$$

$$(D_1)_{p_4} = 2(X_1)_{p_4}(0.268)+(D_1)_p = 7.65 \text{ in}$$

$$(D_2)_p = 2(X_2)_p\ (0.268)+(D_1)_p = 8.50 \text{ in}$$

In the model, as shown in Fig. 15 (b), the corresponding values of $(X_1)_{m_1}$ to $(X_2)_m$ can be defined and calculated as

$$(X_1)_{m_1} = f_s^2 \frac{\pi}{4}(X_1)^2_{p_1} = 0.5\frac{(X_1)^2_{p_1}}{(D_1)^2_{p_1}} = 0.07$$

$$(X_1)_{m_2} = f_s^2 \frac{\pi}{4}(X_1)^2_{p_2} = 0.5\frac{(X_1)^2_{p_2}}{(D_1)^2_{p_2}} = 0.28$$

$$(X_1)_{m_3} = f_s^2 \frac{\pi}{4}(X_1)^2_{p_3} = 0.5\frac{(X_1)^2_{p_3}}{(D_1)^2_{p_3}} = 0.62$$

$$(X_1)_{m_4} = f_s^2 \frac{\pi}{4}(X_1)^2_{p_4} = 0.5\frac{(X_1)^2_{p_4}}{(D_1)^2_{p_4}} = 1.10$$

$$(X_2)_p = f_s^2 \frac{\pi}{4}(X_2)^2_p = 0.5\frac{(X_2)^2_p}{(D_1)^2_p} = 1.75$$

and the respective values of $(A_1)_{m_1}$ to $(A_2)_m$

$$(A_1)_{m_1} = f_s^2 \frac{\pi}{4}(D_2)_{p_1}^2 = 0.5(\frac{5.10}{4.25})^2 = 0.72 \text{ in}^2$$

$$(A_1)_{m_2} = f_s^2 \frac{\pi}{4}(D_1)_{p_2}^2 = 0.98 \text{ in}^2$$

$$(A_1)_{m_3} = f_s^2 \frac{\pi}{4}(D_1)_{p_3}^2 = 1.28 \text{ in}^2$$

$$(A_1)_{m_4} = f_s^2 \frac{\pi}{4}(D_1)_{p_4}^2 = 1.62 \text{ in}^2$$

$$(A_2)_m = f_s^2 \frac{\pi}{4}(D_2)_p^2 = 2.00 \text{ in}^2$$

Therefore, the configuration of the respective analog model will be build as shown in Fig. 15 (b).

4.2 EVALUATION AND COMPARING THE CENTER-LINE VALUES OF VELOCITY AND PRESSURE PERFORMED BY THE PROTOTYPE AND THE MODEL

From the equation of continuity, and under incompressible fluid flow conditions, the center-line values of velocity, as shown in Fig. 16, Fig. 17 and Fig. 18, may be evaluated from the model plottings. The deviations (Dev.), between the results obtained from the electric analog model and that performed by the conventional experiment are as follows:

for $\beta = 15^o$

(Dev.) = 15% max., where $X/D_1 < 10$

(Dev.) = 0, where $X/D_1 > 10$

for $\beta = 90^o$

$$(\text{Dev.}) = 57\% \text{ max.}, \quad \text{where } X/D_1 < 10$$

$$(\text{Dev.}) = 0, \quad \text{where } X/D_1 > 10$$

Physically, the discrepancies existing in the region of separation, say $0 < X/D_1 < 10$, are mainly due to the vortex flow, which cannot be determined by the electrical model. Therefore, a correction of the measurement in the electric analog has to be made.

We now may consider the flow out of the inlet tube as a jet bounded by a conic surface with an angle of β_c, as shown in Fig. 19. For steady flows this conic surface can be taken as the boundary of the flow. In the electric model, the equivalent surface of the conic surface in the prototype should be also considered as the boundary of the electric current. Then the flow area, or the equipotential area, measured in the electric model should be limited by this equivalent surface.

The angle β_c is an unknown function, and has to be so determined, that the results from the electric model can match properly the results of the prototype. For $\beta = 15^o$ and 90^o, the values of β_c are determined as follows:

$$\beta_c = 10^o \quad \text{for} \quad \beta = 15^o$$

and

$$\beta_c = 7^o \qquad \beta = 90^o$$

For the purpose of achievements, transfer the configuration of the correcting angle β_c, into that of the appropriate model plottings, as shown in Fig. 16. The electric analog model tests results being achieved, before and after the corrections may be represented in Figs. 17 and 18. The deviations between them then reduce to

$$(\text{Dev.}) < 2\%, \text{ for } \beta = 15^{\circ}$$

$$(\text{Dev.}) < 1.5\%, \text{ for } \beta = 90^{\circ}$$

For evaluating and comparing the center-line values of pressure performed by the prototype and the model, we may start from eqns. (2.37), (2.38) and (2.39), since

$$\frac{P_1 - P}{\rho g \Delta h_{1\cdot 2}} + \frac{V_1^2}{2g\Delta h_{1\cdot 2}} \left[1 - \left(\frac{A_1}{A}\right)^2\right] = \alpha$$

Dividing each term by $V_1^2/2g\Delta h_{1\,2}$ and rearrange

$$-\frac{P}{\frac{\rho V_1^2}{2}} = \frac{2g\Delta h_{1,2}}{V_1^2}\alpha - \frac{P_1}{\frac{\rho V_1^2}{2}} - 1 + \left(\frac{A_1}{A}\right)^2 \qquad (4.1)$$

in which we set

$$P_1/\rho + V_1^2/2 = \text{constant} = 0$$

at the intake section, then

$$\frac{P_1}{\frac{\rho V_1^2}{2}} = -1 \qquad (4.2)$$

Substituting (4.2) into (4.1), it becomes

$$-\frac{p}{\frac{\rho V_1^2}{2}} = \frac{2g\Delta h_{1.2}}{V_1^2}\,\alpha + \left(\frac{A_1}{A}\right)^2 \qquad (4.3)$$

For $\beta = 90^{\circ}$, the value of $\Delta h_{1\cdot2}$ may be considered, as shown in Fig. 20, from the calculation of two regions (X_p and $L - X_p$), then

$$\Delta h_{1.2} = \Delta h_{xp} + \Delta h_{L-x_p} \qquad (4.4)$$

in which

$$X_p = \frac{(D_2-D_1)/2}{2(0.12278)} = 17.35 \text{ in}$$

and

$$L - X_p = 104 - 17.35 = 86.65 \text{ in}$$

Δh_{xp} = total head loss in the region of X_p (due to vortex flow)

$$= \frac{V_1^2}{2g}\left(1 - \frac{A_1}{A_2}\right)^2 \quad (*)$$

$$= \frac{V_1^2}{2g}\left(1 - \tfrac{1}{4}\right)^2 = \frac{V_1^2}{2g}\left(\frac{9}{16}\right) \qquad (4.5)$$

$$= 0.562\ (V_1^2/2g)$$

(*) The detailed evaluation of head loss, $\Delta h_{1\cdot2}$ in an abrupt enlargement may be seen in Appendix III.

Δh_{L-X_p} = total head loss in the region of $L - X_p$ (due to friction)

$$= f\frac{L - X_p}{D_2}\frac{V_2^2}{2g} = f\frac{L - X_p}{D_2}\left(\frac{A_1}{A_2}\right)^2\frac{V_1^2}{2g} \qquad (4.6)$$

where f = friction factor from the given experimental data,[8] since $R_e = 2 \times 10^5$ at intake section, and the roughness for plastic, e = 0.006 in, and $e/D_2 = 0.0007$ from the relation of friction factor f, Reynolds number R_e, and the roughness e, for commercial pipe,[18] we can find f = 0.0047. Substituting into eqn. (4.6)

$$\Delta h_{L-X_p} = 0.0047\ (86.65/8.50)(V_1^2/2g) = 0.025(V_1^2/2g) \qquad (4.7)$$

Substituting eqns.(4.5) and (4.7) into eqn.(4.4), we have

$$\Delta h_{12} = \Delta h_{X_p} + \Delta h_{L-X_p} = (0.562 + 0.025)(V_1^2/2g) = 0.587\ (V_1^2/2g) \qquad (4.8)$$

For $\beta = 15^\circ$, the corresponding $\beta_c = 10^\circ$, the value of Δh_{12} can be evaluated in the same way as in eqns.(4.4) to (4.8), except that

$$X_p = \frac{(D_2 - D_1)/2}{\tan 10^\circ} = 12.05 \text{ in}$$

$$L - X_p = 104 - 12.05 = 91.95 \text{ in}$$

and where

$$\Delta h_{X_p} = K\frac{V_1^2}{2g}\left(1 - \frac{A_1}{A_2}\right)^2 = 0.45\ (V_1^2/2g) \qquad (4.9)$$

in which K = 0.8 approximately (as shown in Appendix IV), and

$$\Delta h_{12} = f\frac{L - X_p}{D_2}\left(\frac{V_2^2}{2g}\right) = f\ \frac{L - X_p}{D_2}\left(\frac{A_1}{A_2}\right)^2\frac{V_1^2}{2g}$$

$$= 0.0031\ (V_1^2/2g) \qquad (4.10)$$

Substituting eqns. (4.9) and (4.10) into eqn. (4.4), we have

$$\Delta h_{12} = \Delta h_{X_p} + \Delta h_{L-X_p}$$

$$= (0.45 + 0.0031)(V_1^2/2g) = 0.453\left(\frac{V_1^2}{2g}\right) \qquad (4.11)$$

Thus substituting eqns. (4.8) and (4.11) into eqn. (4.3), it becomes

$$-\frac{P}{\frac{\rho V_1^2}{2}} = 0.587\alpha + (A_1/A)^2, \quad \text{for} \quad \beta = 90^\circ \qquad (4.12)$$

$$-\frac{P}{\frac{\rho V_1^2}{2}} = 0.453\alpha + (A_1/A)^2, \quad \text{for} \quad \beta = 15^\circ \qquad (4.13)$$

Furthermore, the values of α which are obtained from the model plottings should be re-evaluated, since the values of α are

$\alpha = 0.125$ at $X/D_1 = 0$; $\alpha = 1.00$ at $L/D_1 = 24.5$ for $\beta = 90^o$

$\alpha = 0.127$ at $X/D_1 = 0$; $\alpha = 1.00$ at $L/D_1 = 24.5$ for $\beta = 15^o$

as shown in Fig. 16. As mentioned in the experimental procedure and in the evaluation of eqns. (4.12) and (4.13), the values of α should be replaced by

$$\alpha_c = \frac{\alpha-0.125}{1.00-0.125} = \frac{\alpha-0.125}{0.875}, \quad \text{for } \beta = 90^o \qquad (4.14)$$

$$\alpha_c = \frac{\alpha-0.127}{1.00-0.127} = \frac{\alpha-0.127}{0.873}, \quad \text{for } \beta = 15^o \qquad (4.15)$$

As shown in Fig. 16, the corresponding values of α that are used in the evaluation of α_c are as follows, for

$\beta = 90^o$

X/D_1	0	1	2	3	4	5	6	7	8	9
α	.125	.167	.205	.245	.283	.322	.358	.395	.430	.473
α_c	0	.050	.090	.138	.180	.225	.266	.310	.350	.399

X/D_1	10	11	12	13	14	15	16
α	.508	.544	.578	.613	.647	.681	.714
α_c	.436	.500	.5.8	.557	.596	.626	.673

for $\beta = 15^{o}$

X/D_1	0	2	3	4	5	6	7	8	9
α	.127	.213	.263	.300	.329	.363	.385	.426	.460
α_c	0	.100	.156	.200	.230	.270	.310	.340	.380

X/D_1	9	10	11	12	13	14	15	16
α	.498	.532	.564	.597	.630	.664	.698	.729
α_c	.425	.468	.500	.539	.578	.615	.655	.690

With the evaluation from eqns. (4.12) and (4.13), accompanied with the appropriate equation (2.14) or (2.15), the deviations of the results performed by the model plottings and the stagnation tube and the pitot tube measurements, are as shown in Figs. 21 and 22.

(Dev.) < 1.5% for $\beta = 90^{o}$

(Dev.) < 1.0% for $\beta = 15^{o}$

4.3 CHECKING RESULTS OBTAINED WITH THE APPLICATION OF THE CORRECTED GRADUATE ANGLE β_c FOR THE PROTOTYPE $\beta = 45^{o}$

Using the same prototype configuration except $\beta = 45^{o}$, applying the same experimental procedure as the aforegoing mentioned, the respective value β_c may be matched from

that being obtained by the graduate angle $\beta = 15^{o}$ and 90^{o}, as follows: since $\beta = 10^{o}$ and 7^{o}, for $\beta = 15^{o}$ and 90^{o}, respectively, it can reasonably be assumed that there is a linear relation between β and β_c, as shown in Fig. 23. Then the value β_c, for $\beta = 45^{o}$, which can be obtained graphically,or calculated, is equal to 8.8^{o}, or 8^{o} 48'.

Applying the same consideration from eqn. (4.1) to the appropriately developed eqn. (4.13), in addition, with the appropriate placement of α_c in line with α according to the electric plottings in Fig. 24, the results are shown in Figs. 24, 25 and 26, and the deviations of V/V_1, and $-\frac{P}{\frac{\rho V_1^2}{2}}$, along the axial direction between the model and the prototype as seen, are both less than 1.5%.

CHAPTER V

CONCLUSIONS

CHAPTER V

CONCLUSIONS

From the above analytical and experimental results, the following conclusions can be made:

1) The velocity and pressure distributions of an incompressible flow through an axial symmetric system with losses can be investigated by using an electrical analog with field plot provided that the information of the total loss across the flow system is available.

2) For flows through a sudden enlargement, there exists vortices, for which there is no analog between the flow system and the electrical system. For such a case, a correction according to Fig. 23 has to be used.

3) The velocity and pressure distributions of an incompressible flow along the axes of tubes with different enlargments obtained by the electrical analog are in alignment with those obtained by the experiments of pitot tube measurements. The maximum error between these two results is about 2%.

4) The electrical analog method developed is especially useful for measuring the velocity and pressure distributions in small complicated flow systems, such as fluid control devices, to which other methods may be difficult to apply.

REFERENCES

REFERENCES

[1] Murphy, G., Similitude in Engineering, Ronald Press Co., (1950).

[2] Langhaar, H.L., Dimensional Analysis and Theory of Models, John Wiley and Sons, Inc., New York, (1951).

[3] Liebmann, G., Electrical Analogues, Grit. Journal of Applied Physics, Vol. 4, (1953).

[4] Ross, G.S., and Qureshi, I.H., Boundary Value Problems in Two-Dimensional Electricity by Conducting Paper Analogue, Journal of Scientific Instrument, Vol. 40, (November, 1963).

[5] Surowiak, S., The Solution of Distributed Source Field Problems with the Conducting Paper Analogue, AEI Engineering (May/June, 1965).

[6] Letham, D.L., Fluidic System Design, Machine Design, Penton Publications, Vol. 38, (1966).

[7] Kirshner, J.M. Fluid Amplifiers, McGraw-Hill Book Co., (1966).

[8] Chaturvedi, M.C., Flow Characteristics of Axisymmetric Expansions, Journal of the Proceedings, ASCE, HY-3, (May 1963)

[9] Shapiro, A., The Dynamics and Thermodynamics of Compressible Fluid Flow, The Ronald Press Co., Vol. 1, (1953).

[10] Williams, F.A., Linearized Analysis of Constant Property Duct Flows, Department of Aerospace and Mechanical Engineering Seminar, University of California, San Diego, La Jolla, California, (May, 1968).

[11] Krishnaiyer, R., and Lechner, T.J. Jr., An Experimental Evaluation of Fluidic Transmission Line Theory, Advances in Fluidics, ASME, (1967).

[12] Brychta, O., The Digital System Using Microdiaphragm-Ejector Amplifier and Its Use in Automation, SGWU Paper, (1970).

[13] Enzo, O., and Hung, T.K., Computational and Experimental Study of a Captive Annular Eddy, Journal of Fluid Mech. Vol. 28, (1967).

[14] Rouse, H., and Kalin, T.T., Turbalance Characteristics of Hydraulic Jump, Trans. ASCE, Vol. 124, (1959).

[15] Catmody, T.J., Effect of Turbulence on Conventional Static and Total Head Tube, Iowa Inst. of Hydr. Research, Iowa City, Iowa, (1962).

[16] Vennard, J.K., Elementary Fluid Mechanics, John Wiley & Sons, Inc., 4th Edition, (1962).

[17] Salaman Eskinazi, Principles of Fluid Mechanics, 2nd Edition, Allyn and Bacon, Inc., (1968).

[18] Moody, L.F., Friction Factors for Pipe Flow, Trans. ASME, Vol. 66, (1944).

DRAWINGS

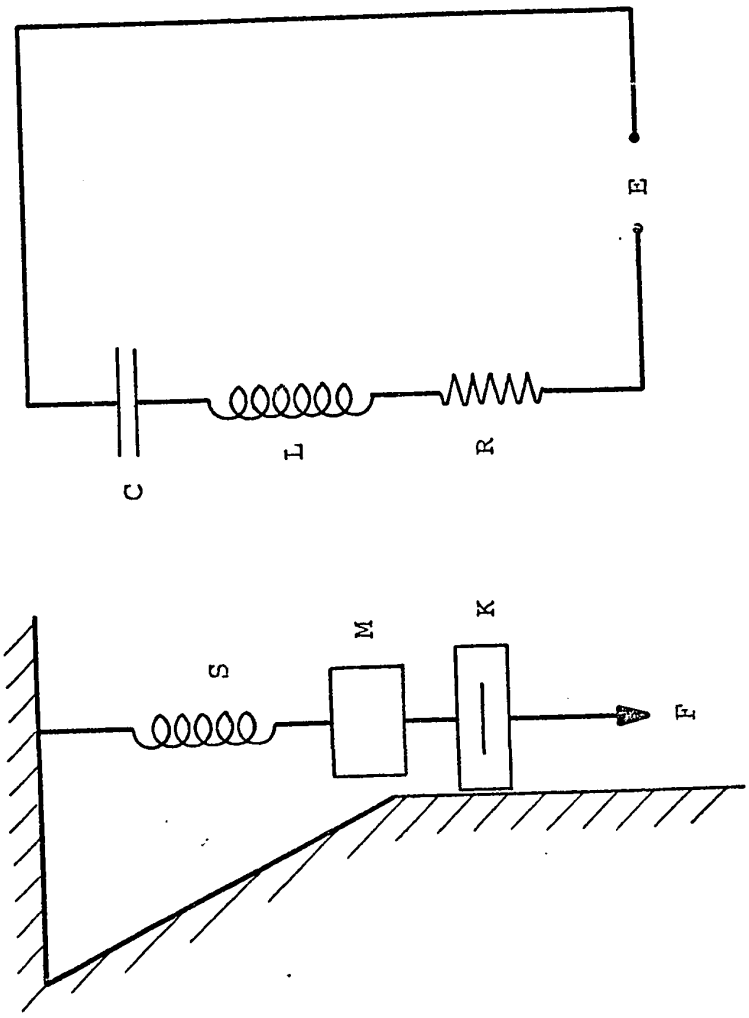

FIG. 1 Mechanical System and Analogous Electrical System

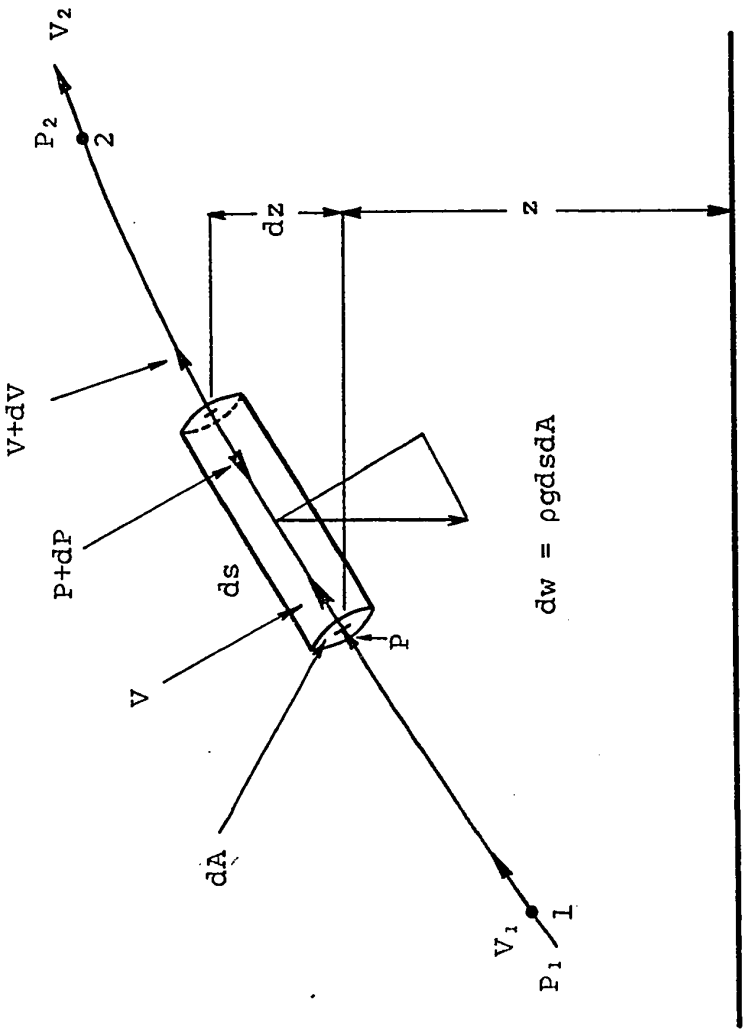

FIG. 2 Differential Element of Fluid Flow-One-Dimensional

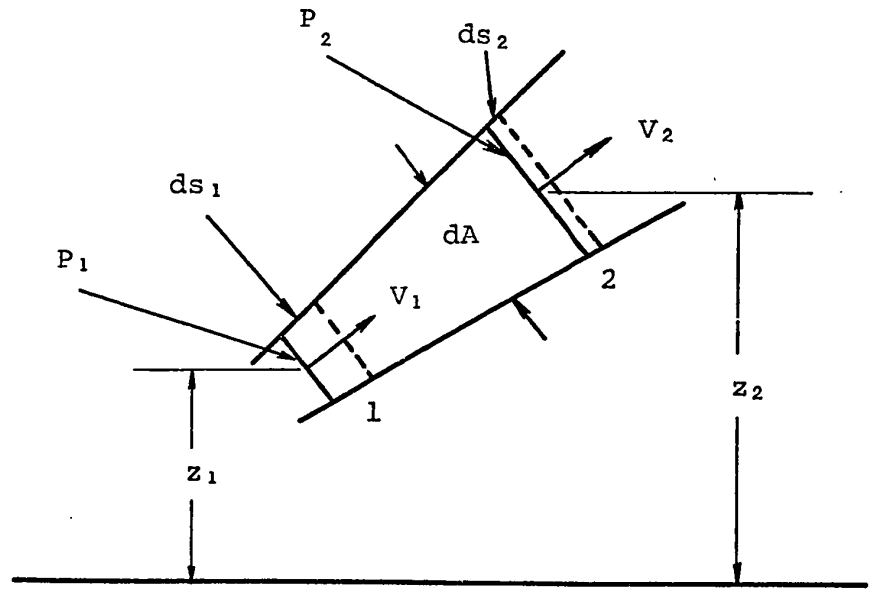

FIG. 3 Energy Displacement Carried by Fluid Flow

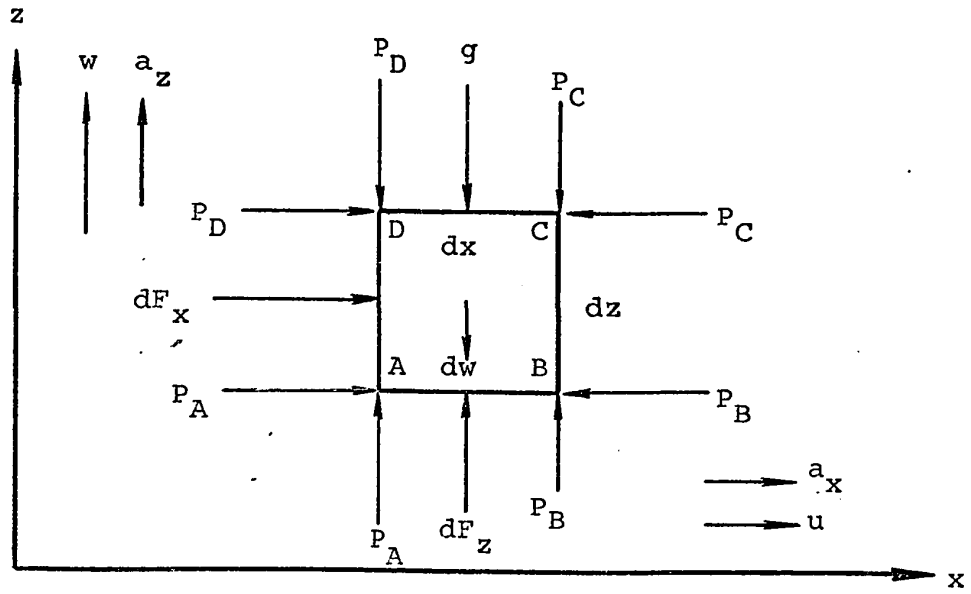

FIG. 4 Differential Element of Fluid Flow - Two-Dimensional

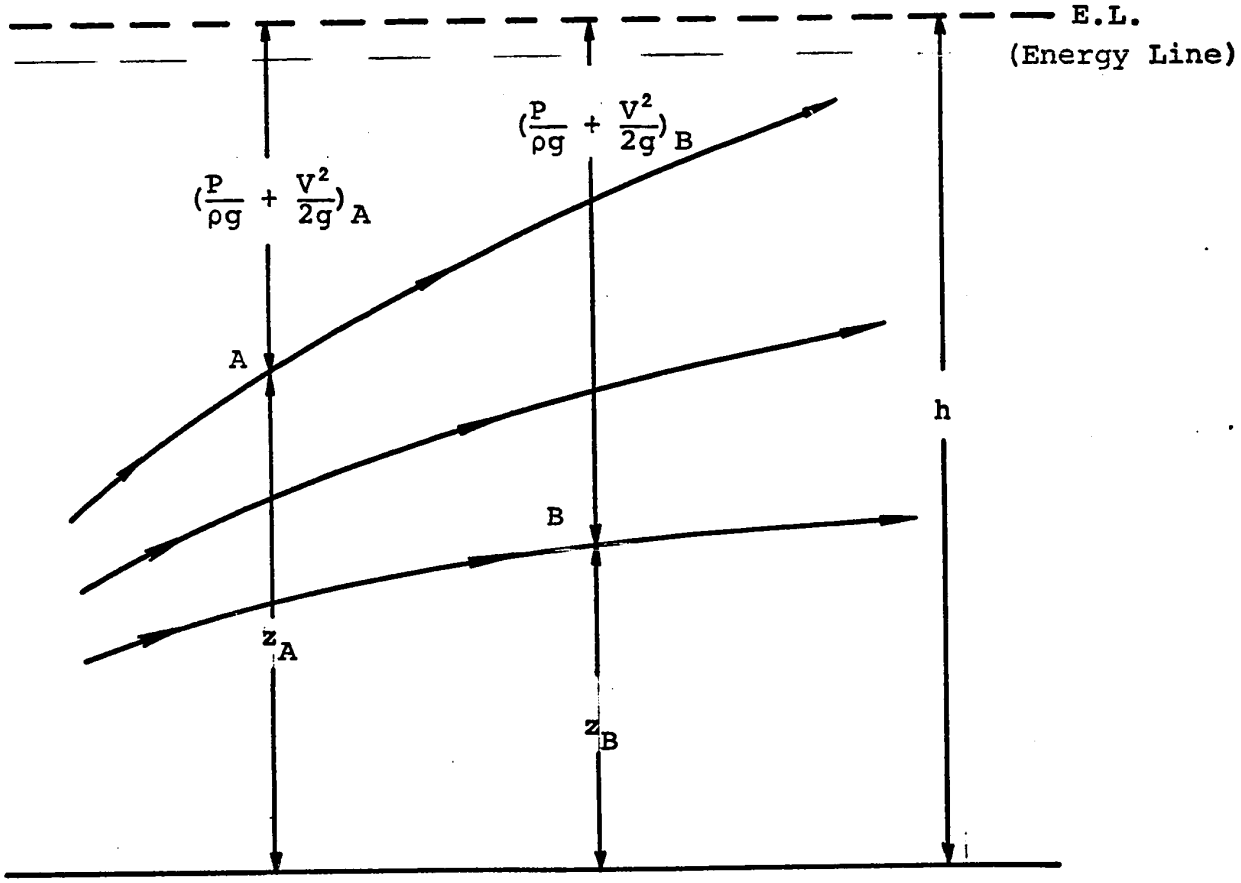

FIG. 5 Energy Line for Fluid Flow

Fluid Mechanical Energy Difference:

$$\left(\frac{P}{\rho}+\frac{V^2}{2}+zg\right)_1 - \left(\frac{P}{\rho}+\frac{V^2}{2}+zg\right)_2 = g\Delta h_{1,2}$$

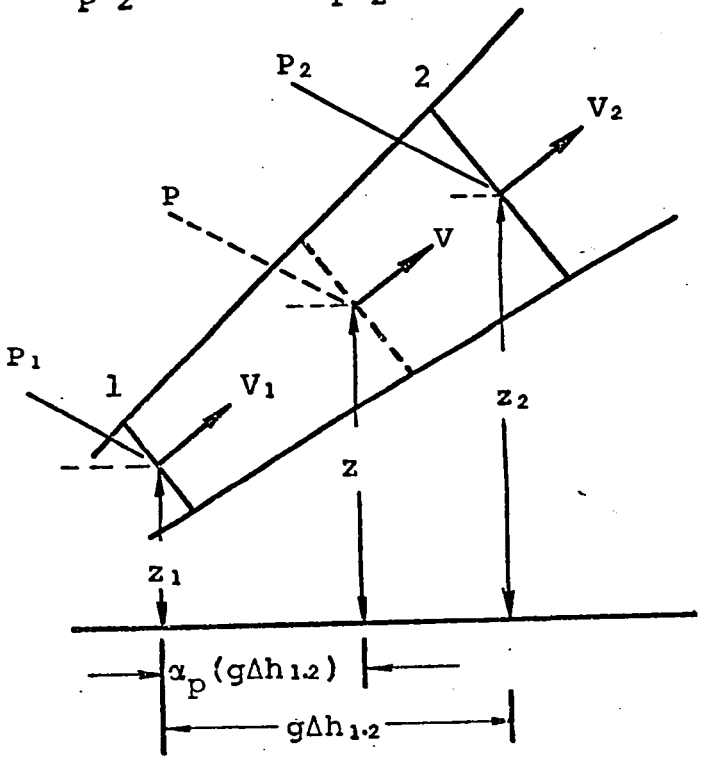

Electrical Potential Voltage Difference:

$$e_1 - e_2 = \Delta e_{1\,2}$$

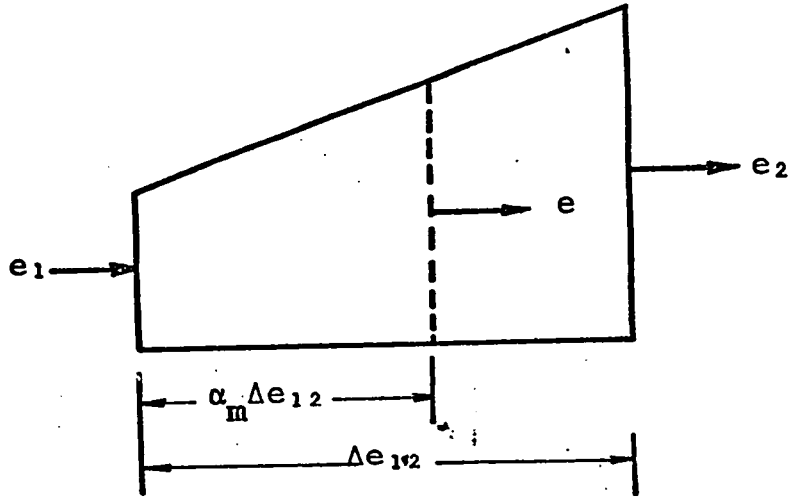

FIG. 6 The Resemblance Sketching of Fluid/Electric Analog

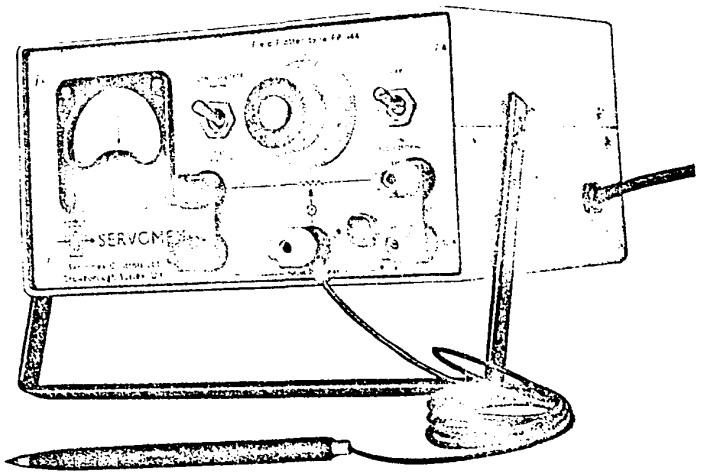

SPECIFICATION

● Instrument Accuracy	0.1%
● Outputs	5-10 V 50-100 V
● Input	100-250 V 45-65 cps
● Consumption	10 VA approx

FIG. 7 The Servomex Field Plotter

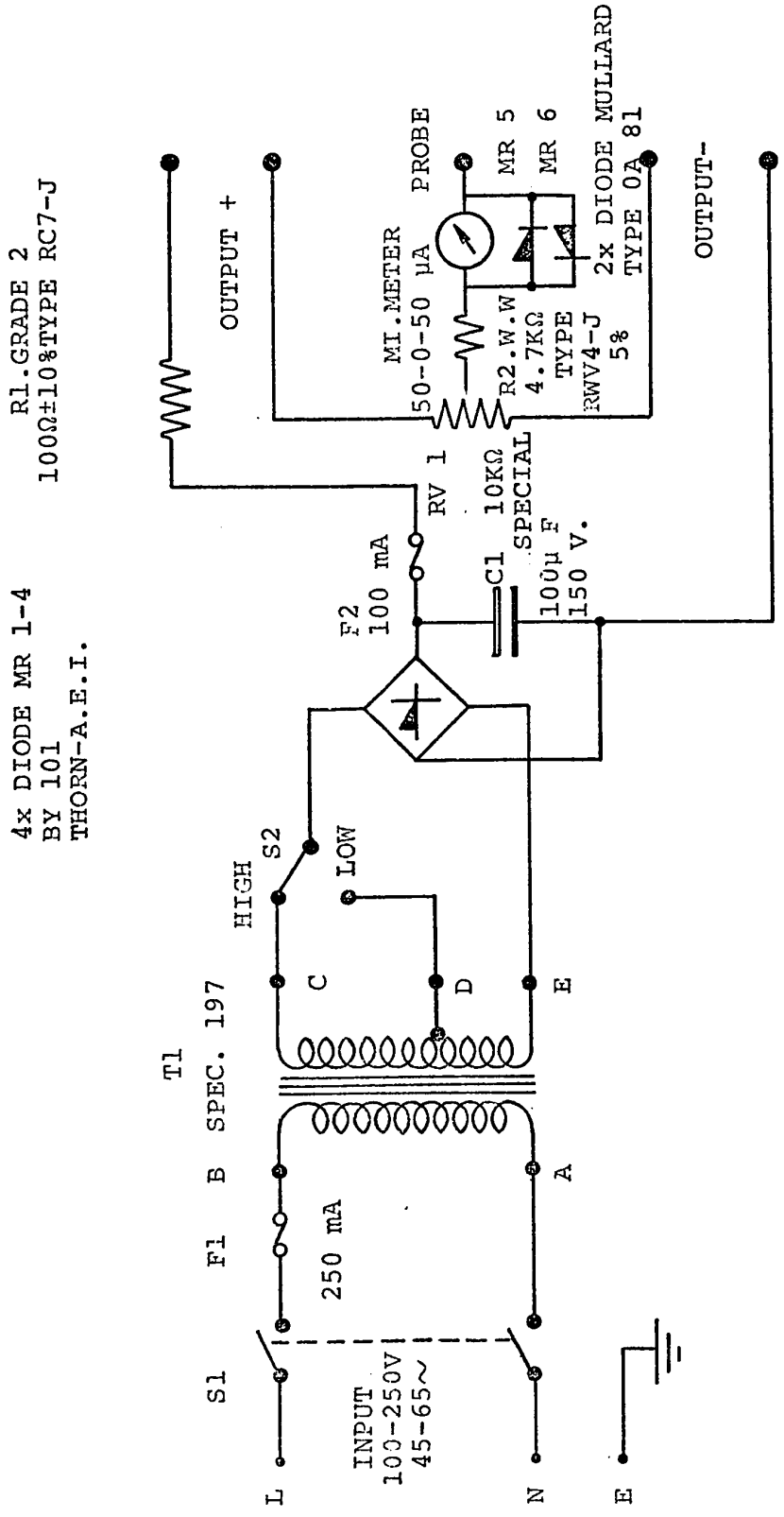

FIG. 8 The Electric Circuit Diagram of Field Plotter

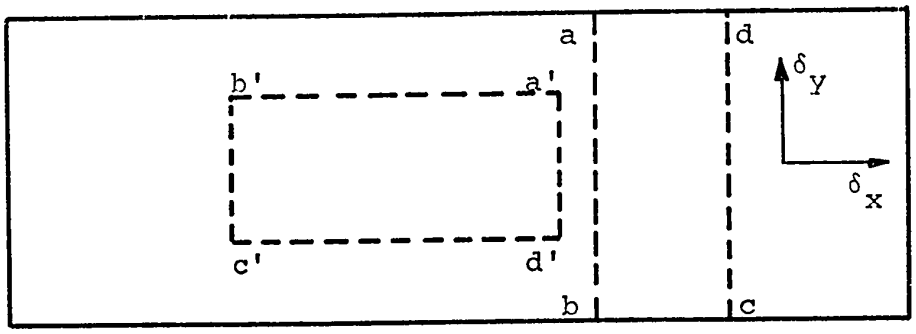

FIG. 9 Ways of Cutting Two Strips of Resistance Paper of Equal Width from Along and Across the Roll

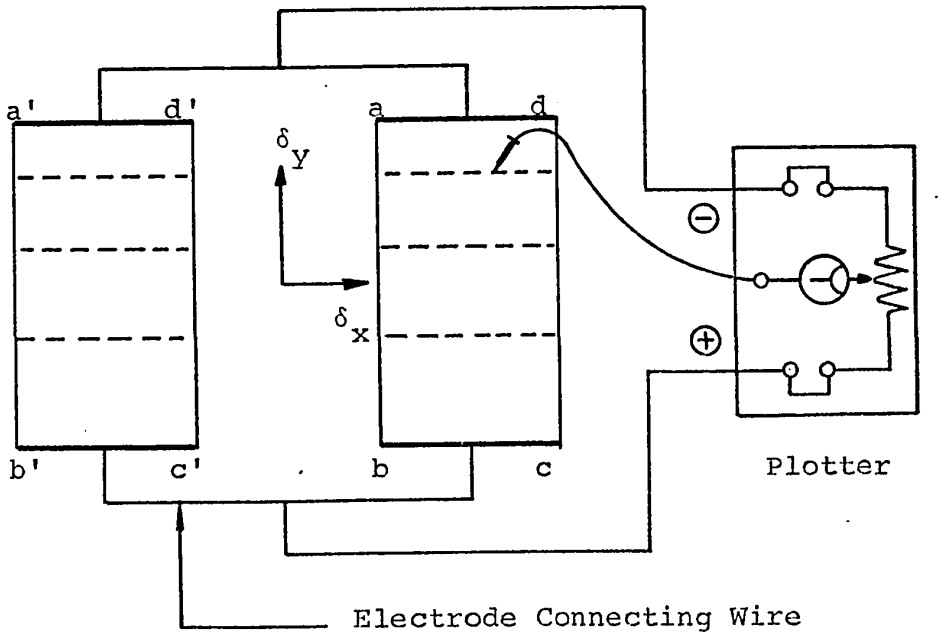

FIG. 10 Ways of Measuring the Potential of Two Strips of Resistance Paper with the Probe

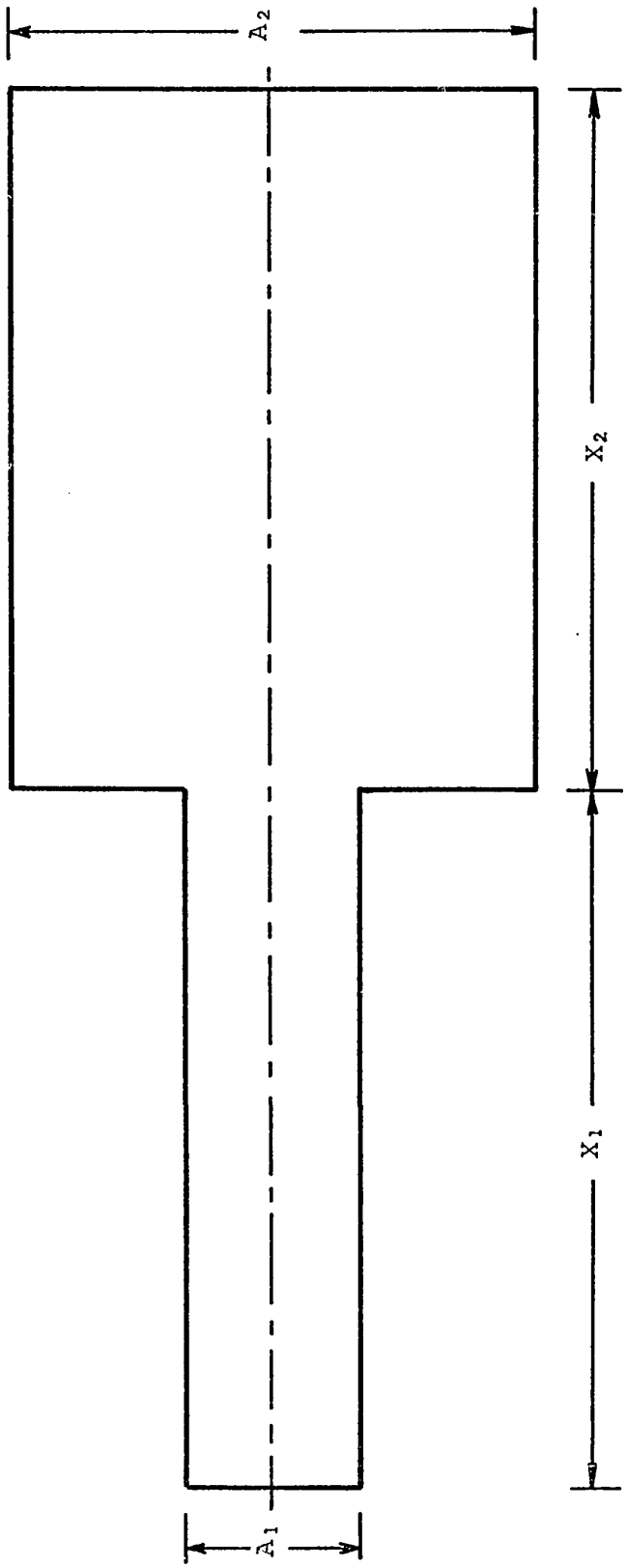

FIG. 11 The Electric Analog Model of an Abrupt Enlargement

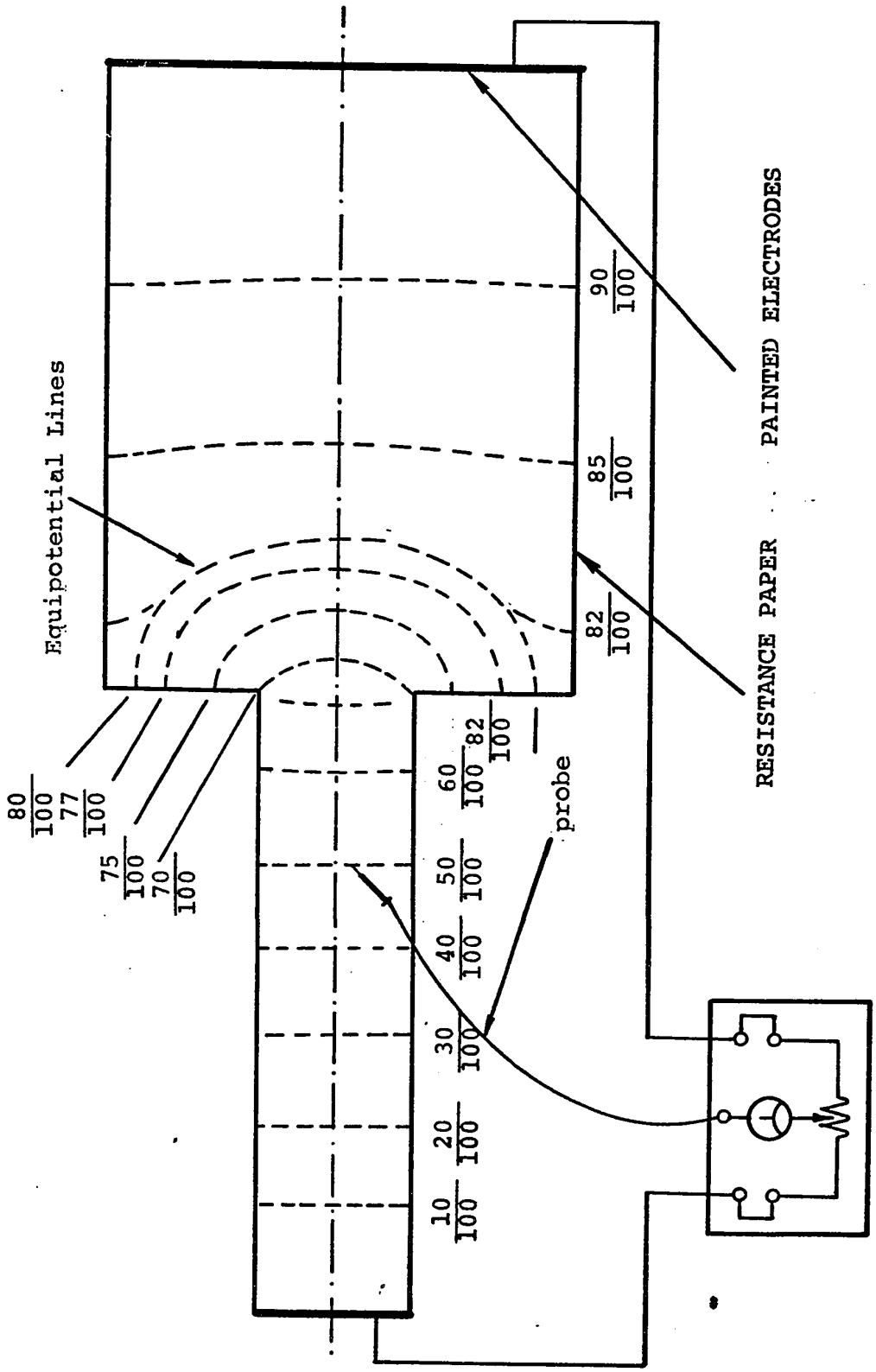

FIG. 12 Electric Model Plottings

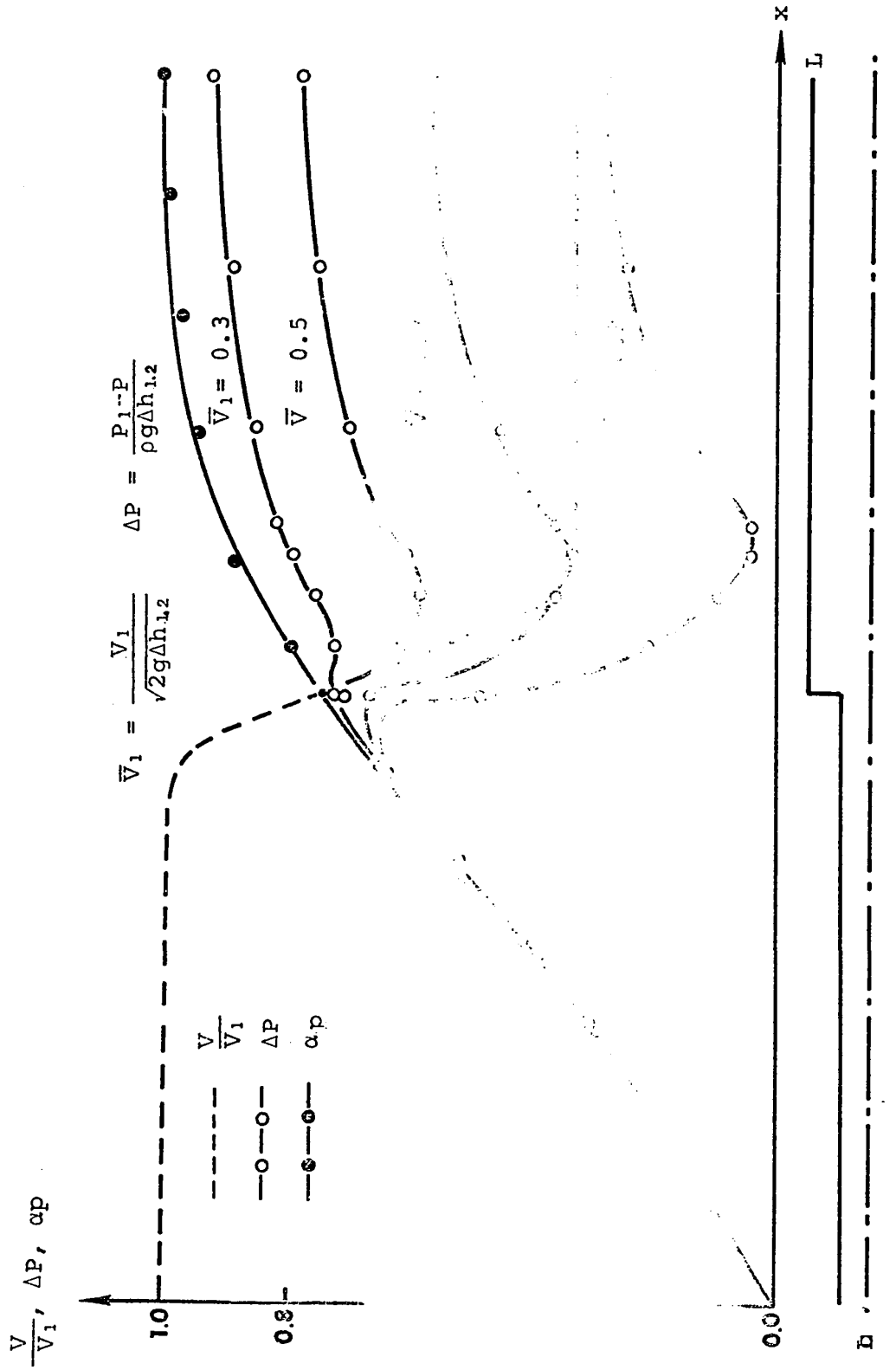

FIG. 13 The Center-Line Values of Velocity and Pressure Along The Axial Direction

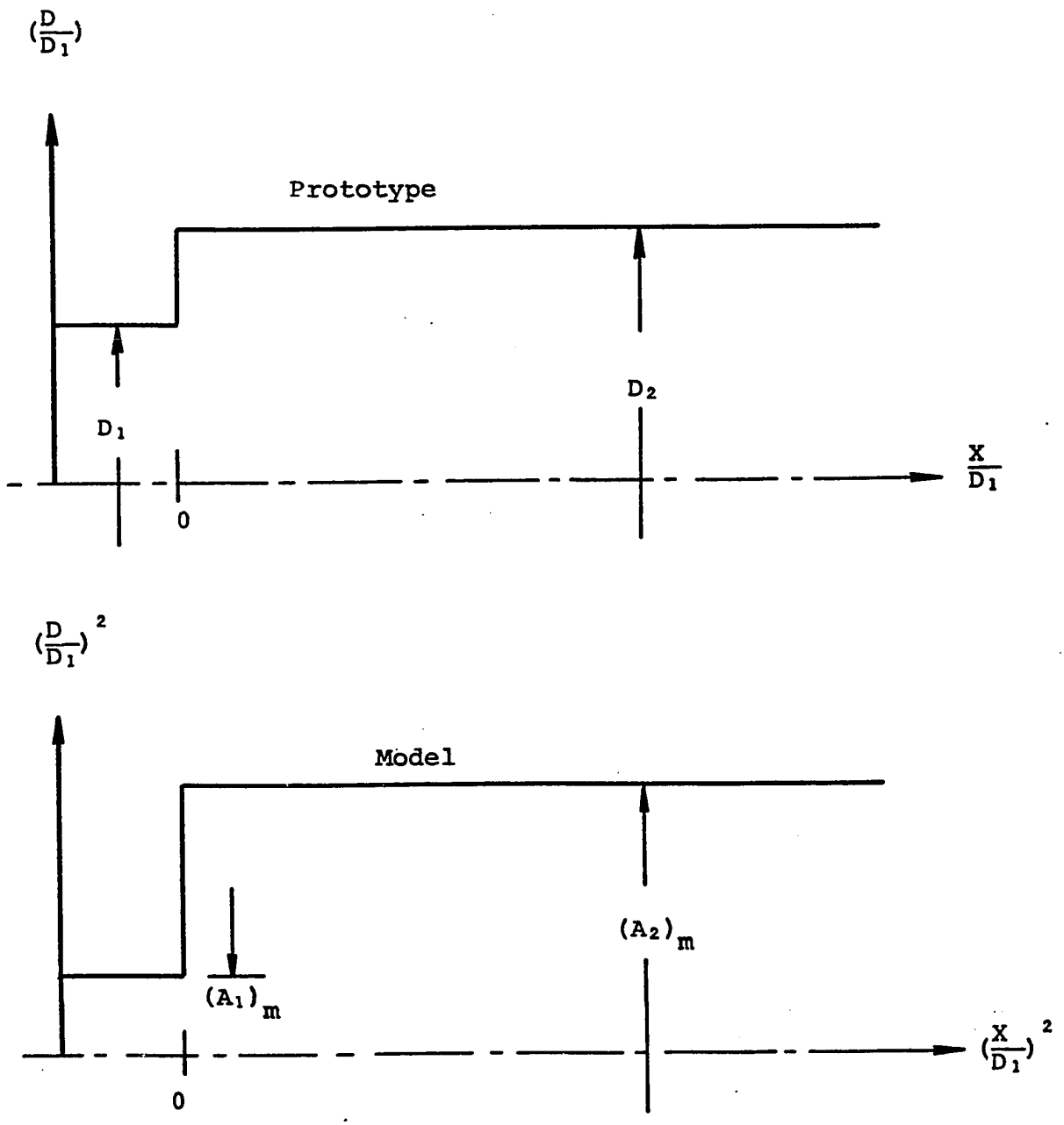

FIG. 14 The Dimensions of the Prototype and the Respective Analog Model

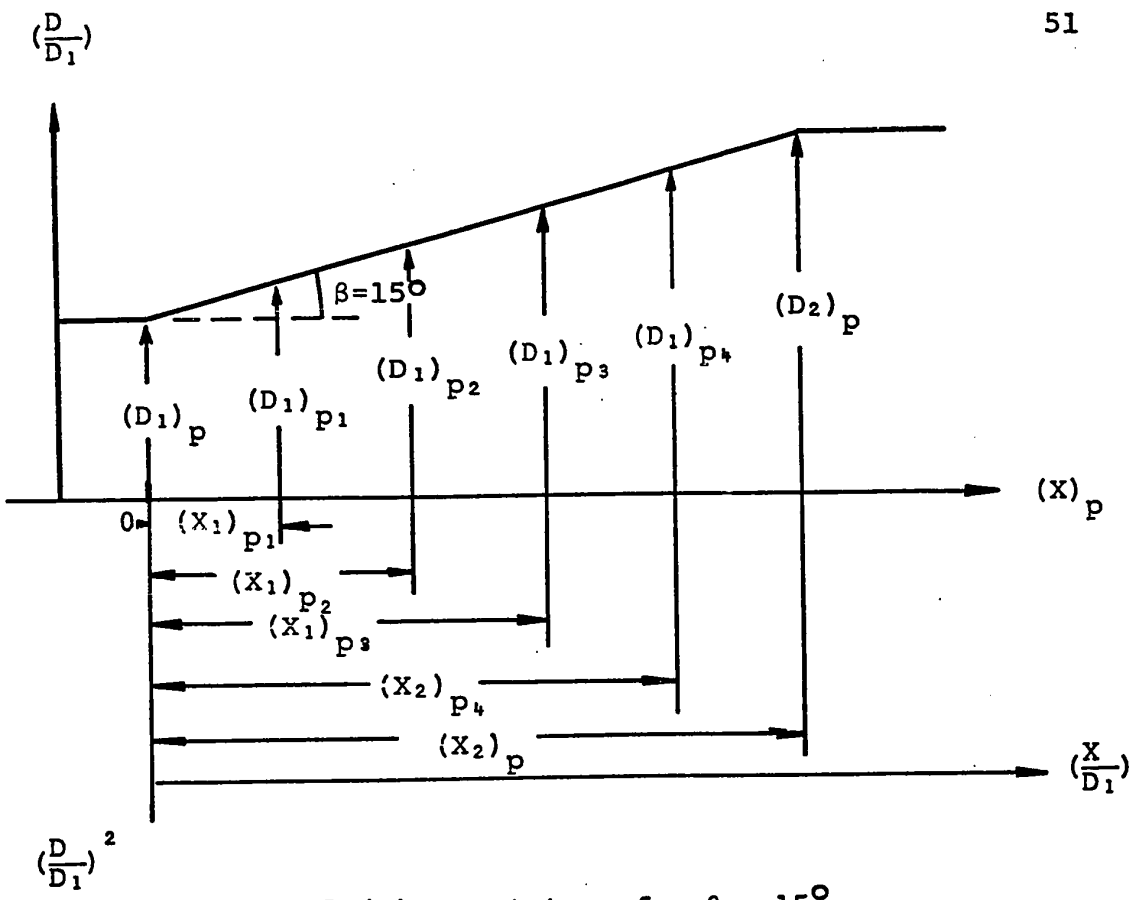

FIG. 15 (a) Prototype, for $\beta = 15^0$

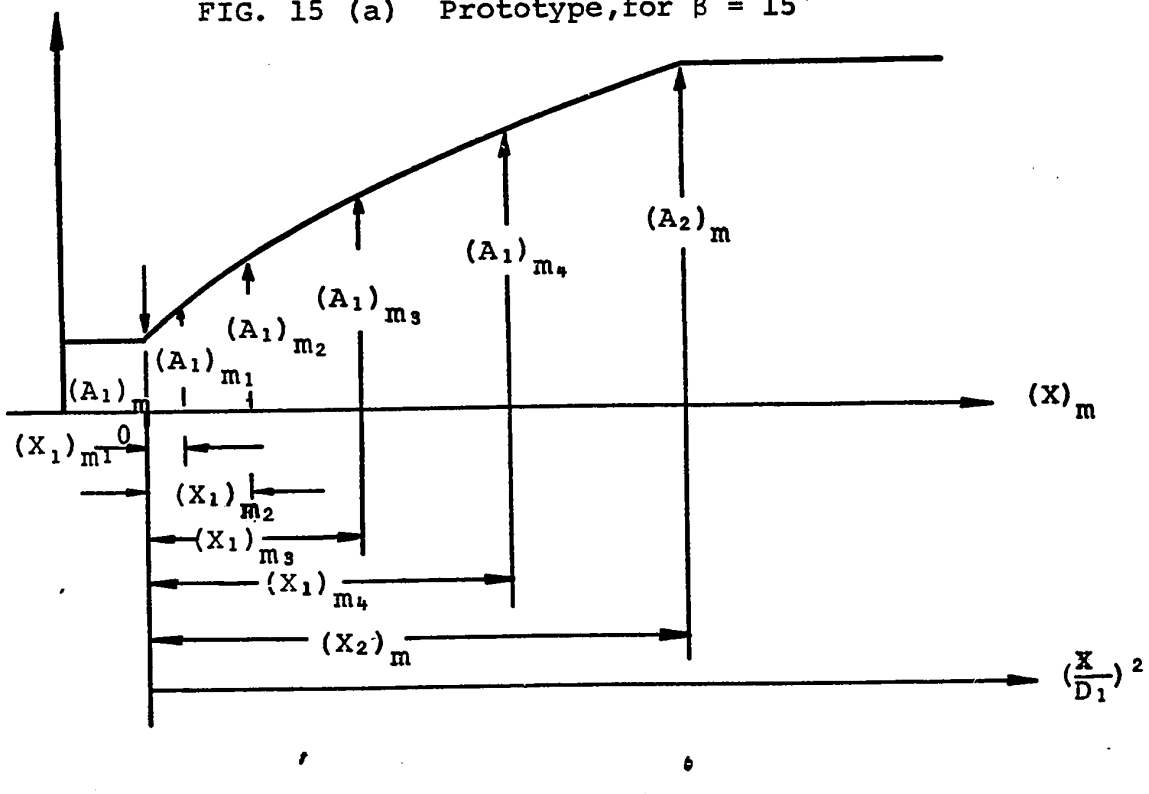

FIG. 15 (b) Analog Model, for $\beta = 15^0$

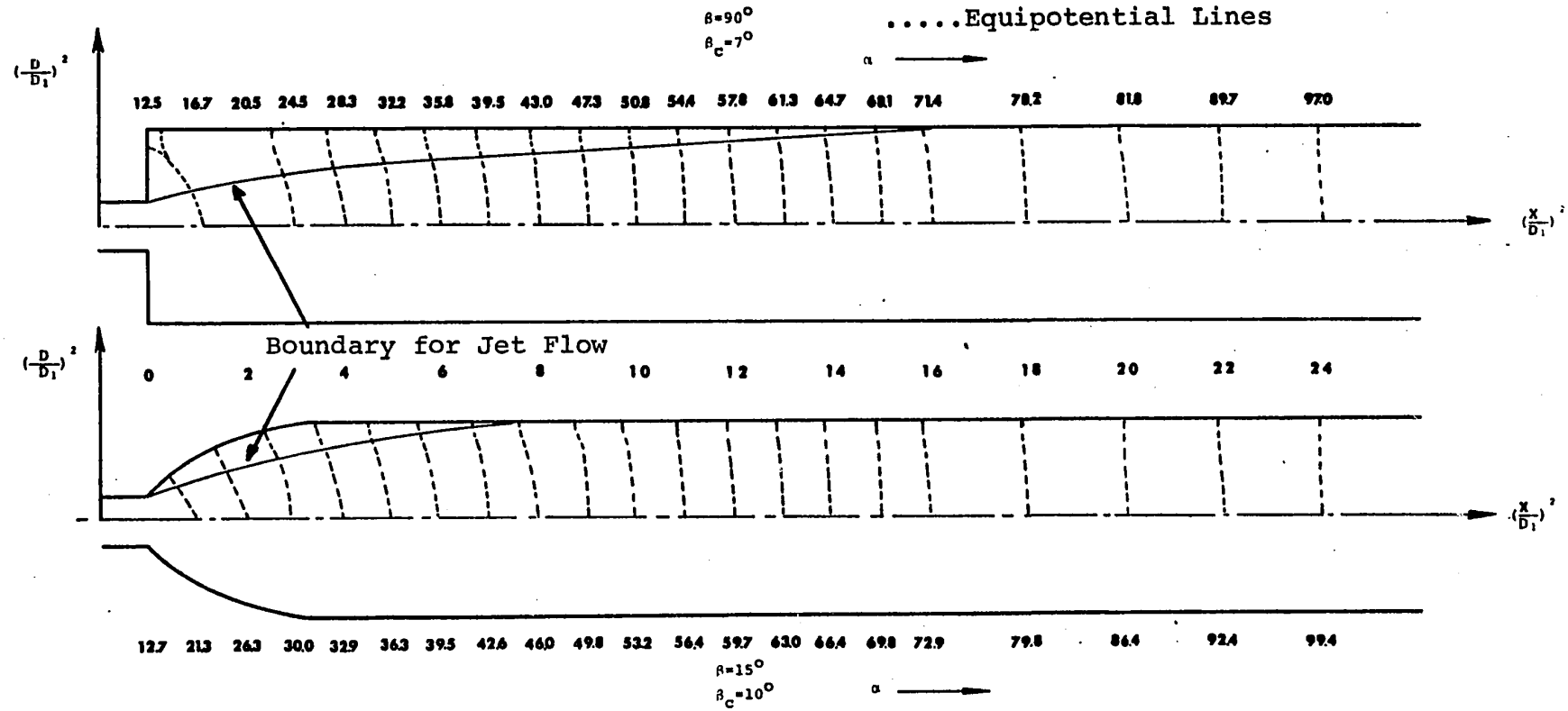

FIG. 16 The Electric Analog Model Plottings, for $\beta = 15^\circ$ and $\beta = 90^\circ$

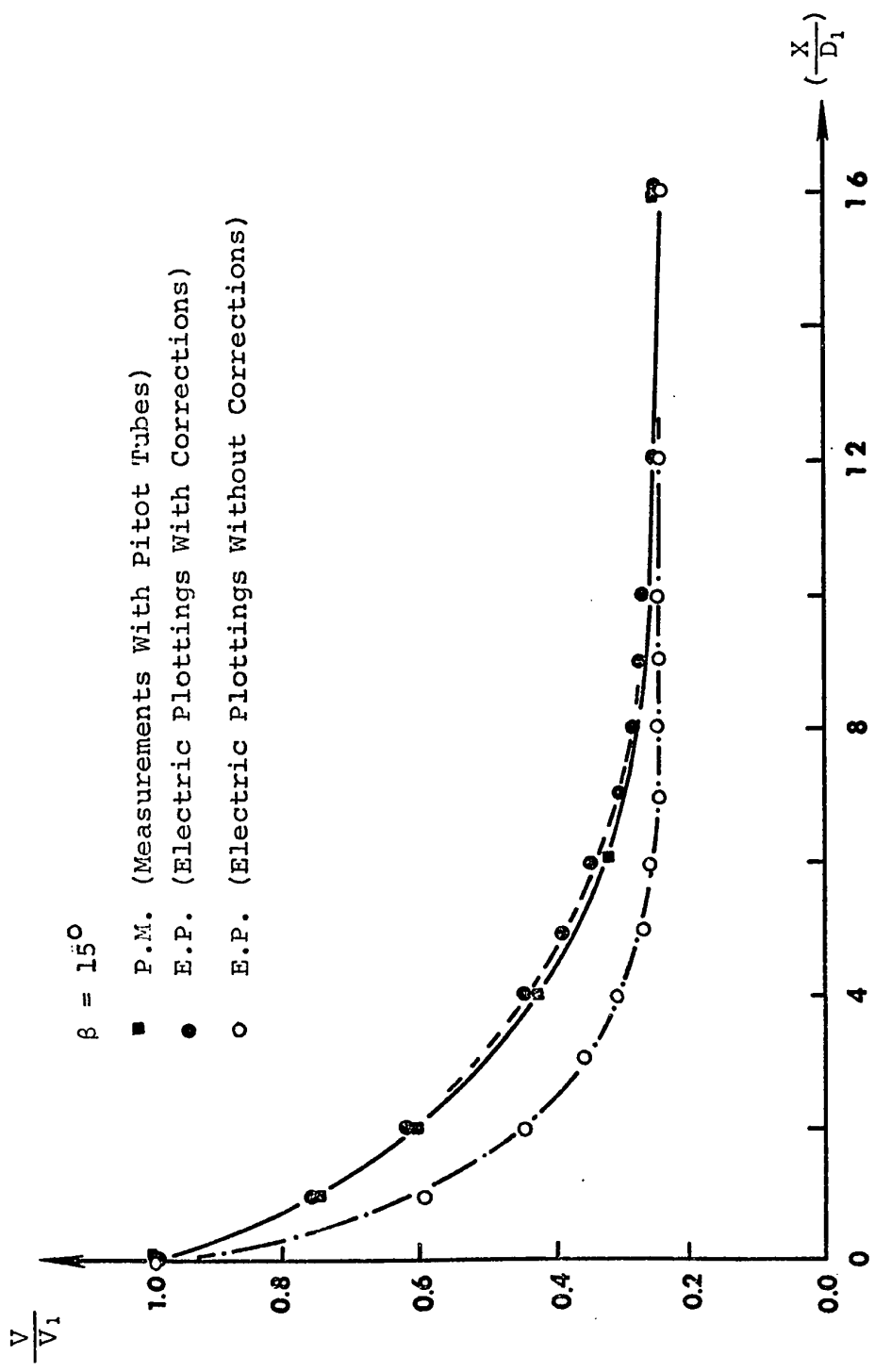

FIG. 17 The Center-Line Value of Valocity, for $\beta = 15^{\circ}$

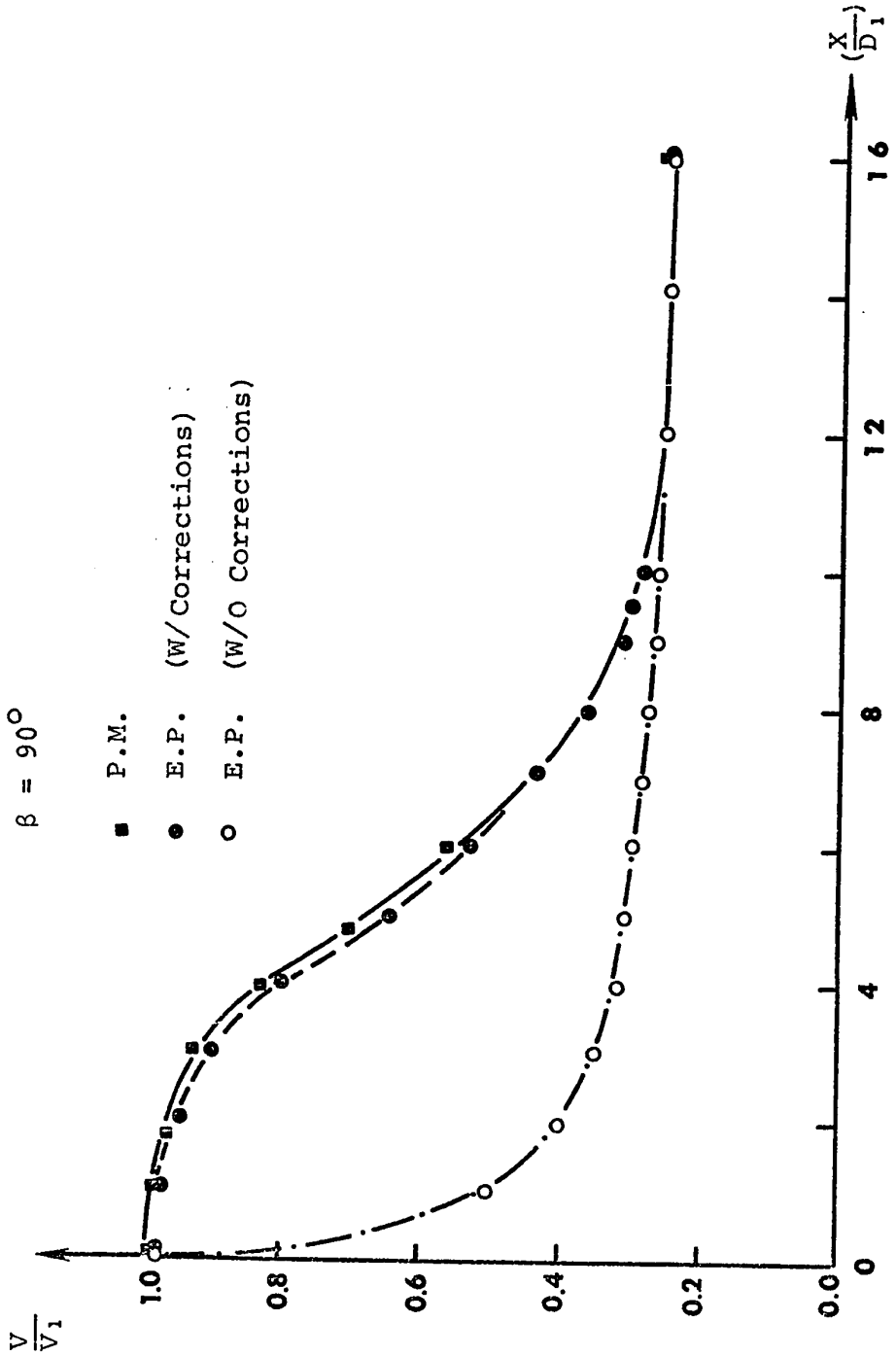

FIG. 18 The Center-Line Value of Velocity, for $\beta = 90^{\circ}$

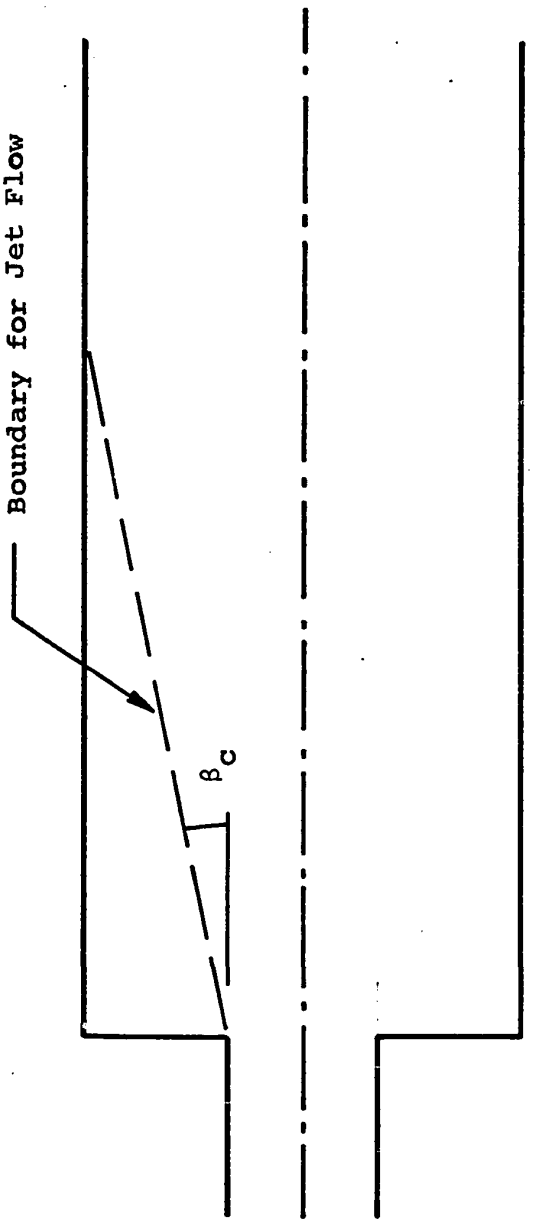

FIG. 19 The Graduate Angle β_c of Placement in the Region of Separation

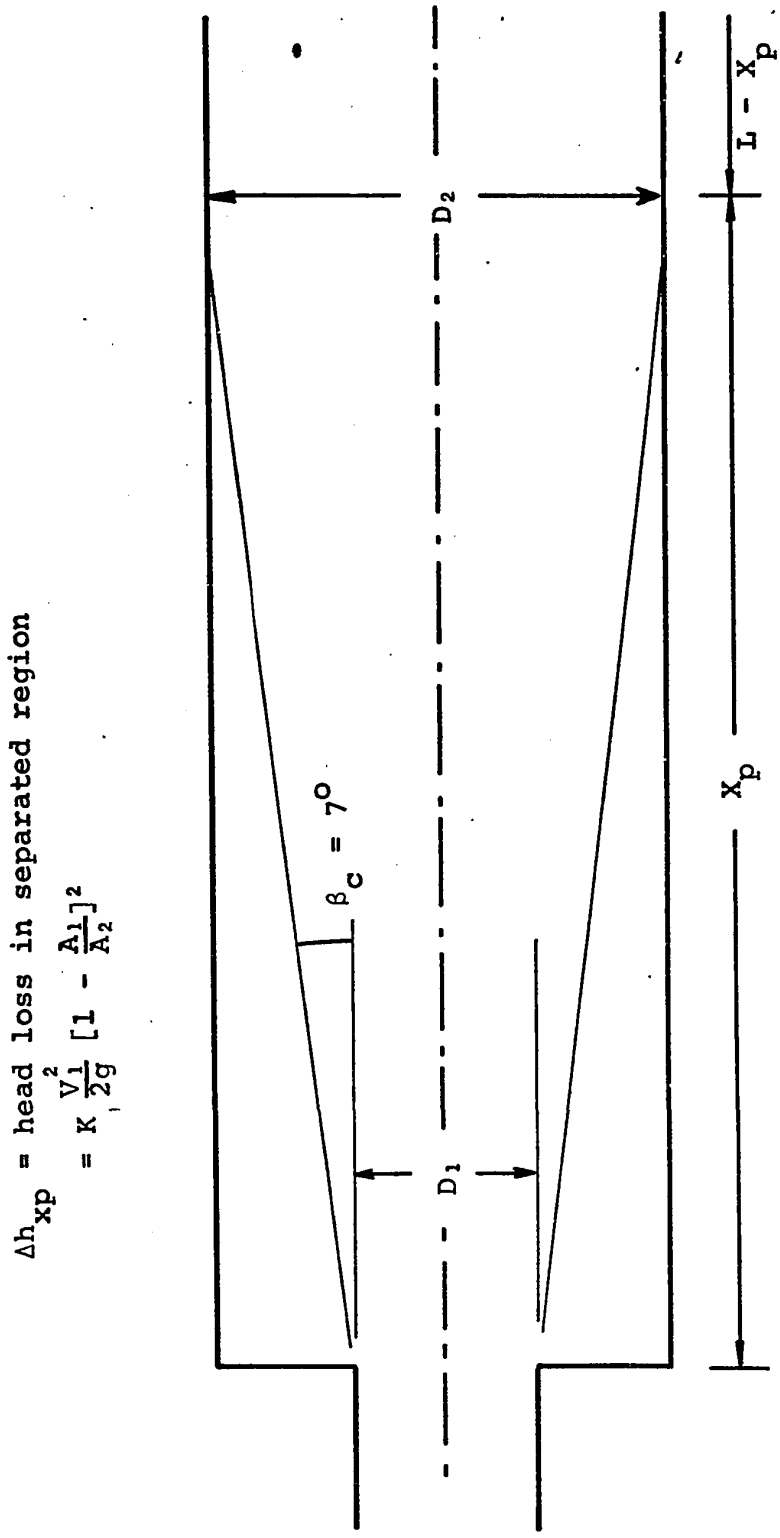

FIG. 20 Evaluation of Head Loss in Separated Regions of Fluid Flow

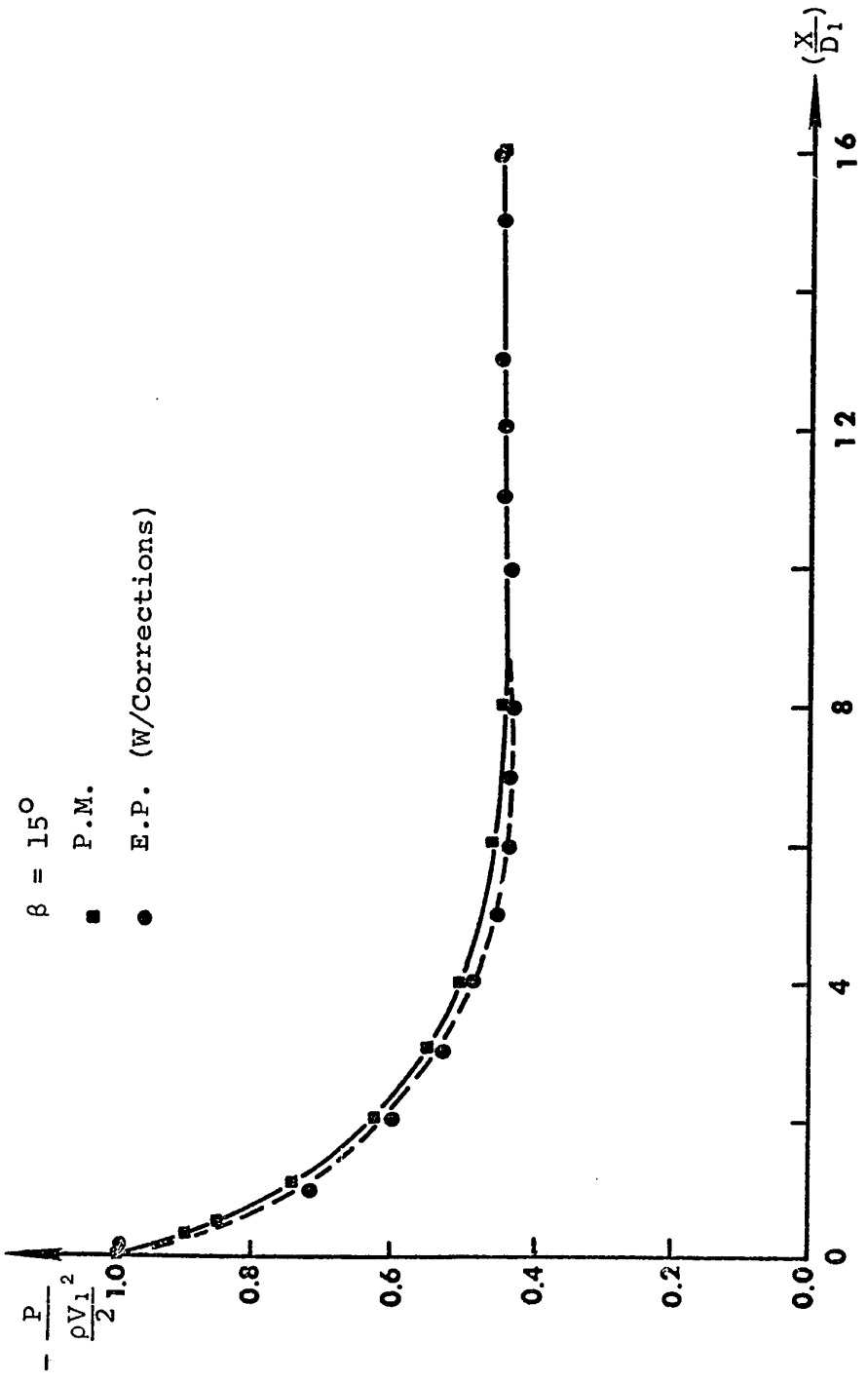

FIG. 21 The Center-Line Value of Pressure, for β = 15°

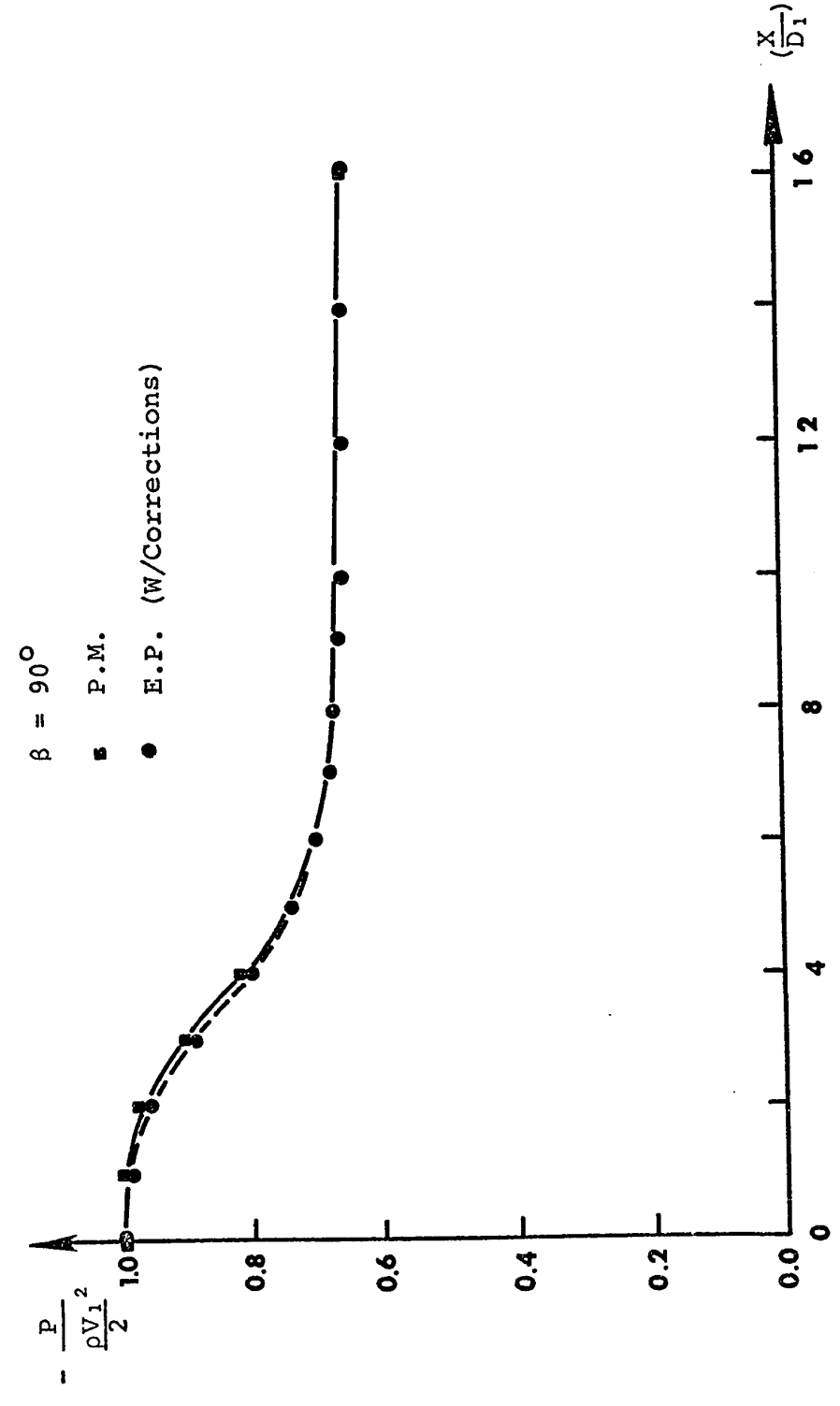

FIG. 22 The Center-Line Value of Pressure, for β = 90°

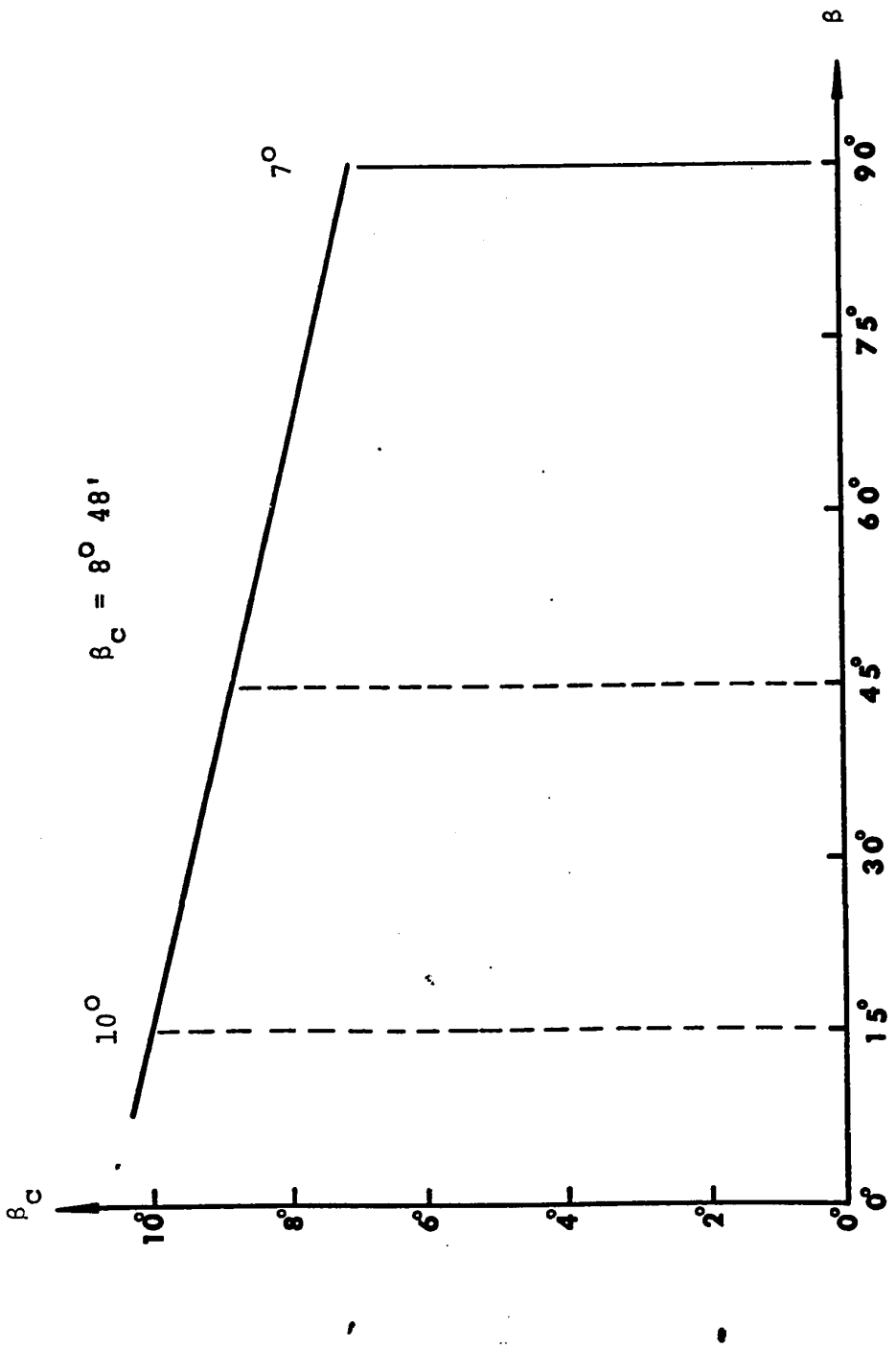

FIG. 23 The Relationship Between β and β_c

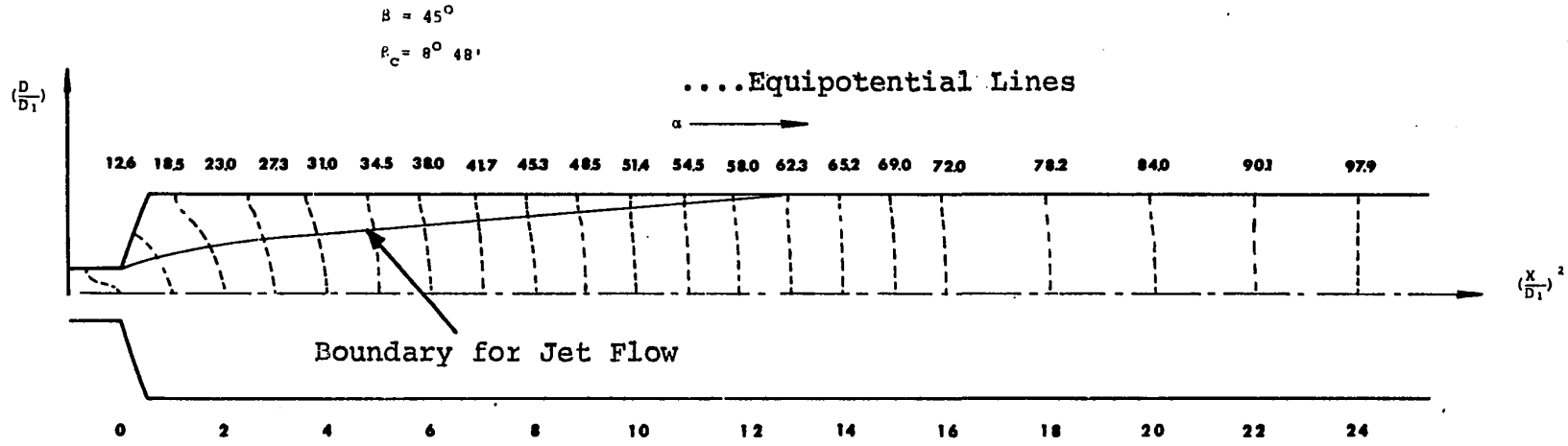

FIG. 24 The Electric Analog Model Plottings, for $\beta=45^{\circ}$

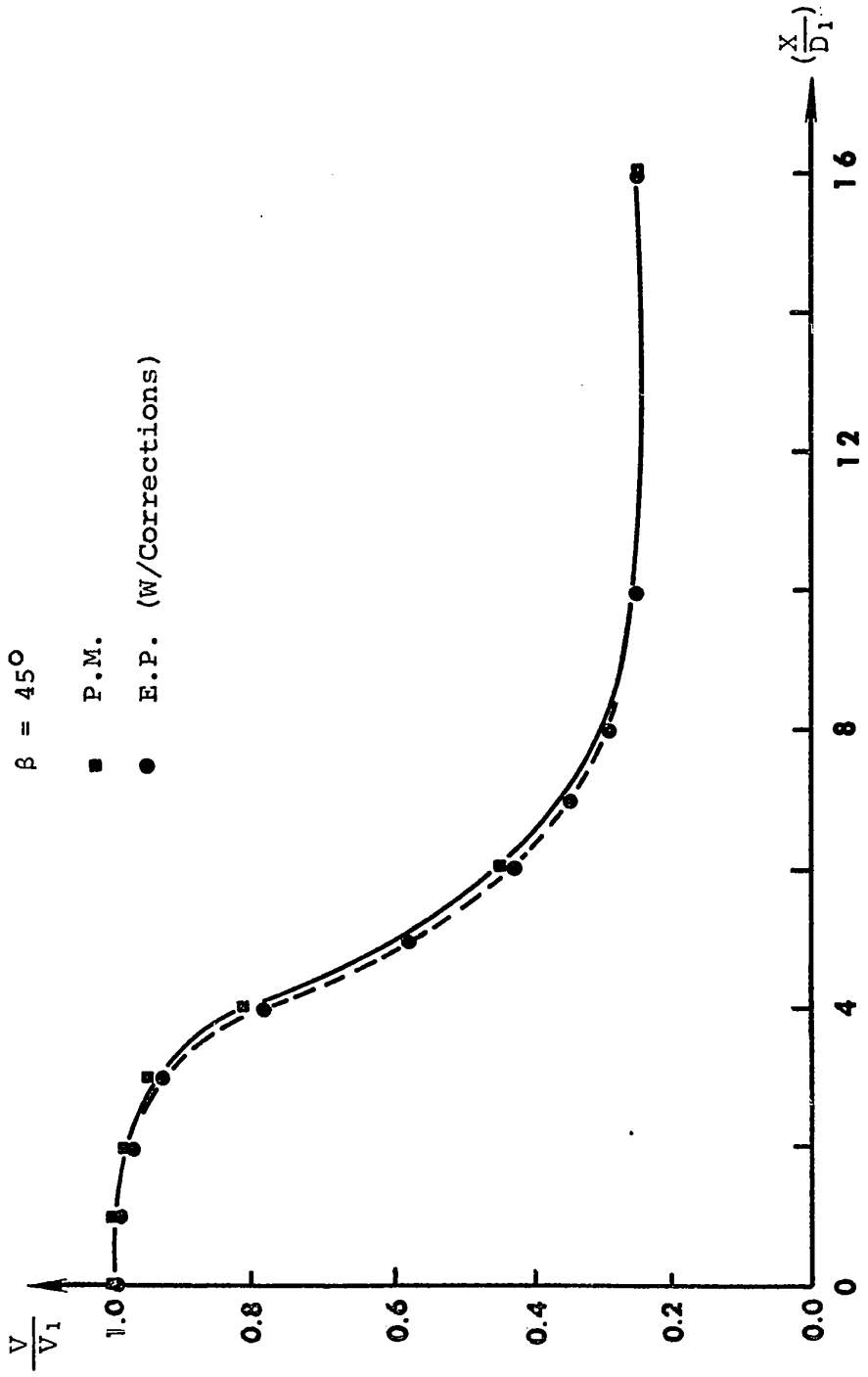

FIG. 25 The Center-Line Value of Velocity, for $\beta = 45^{\circ}$

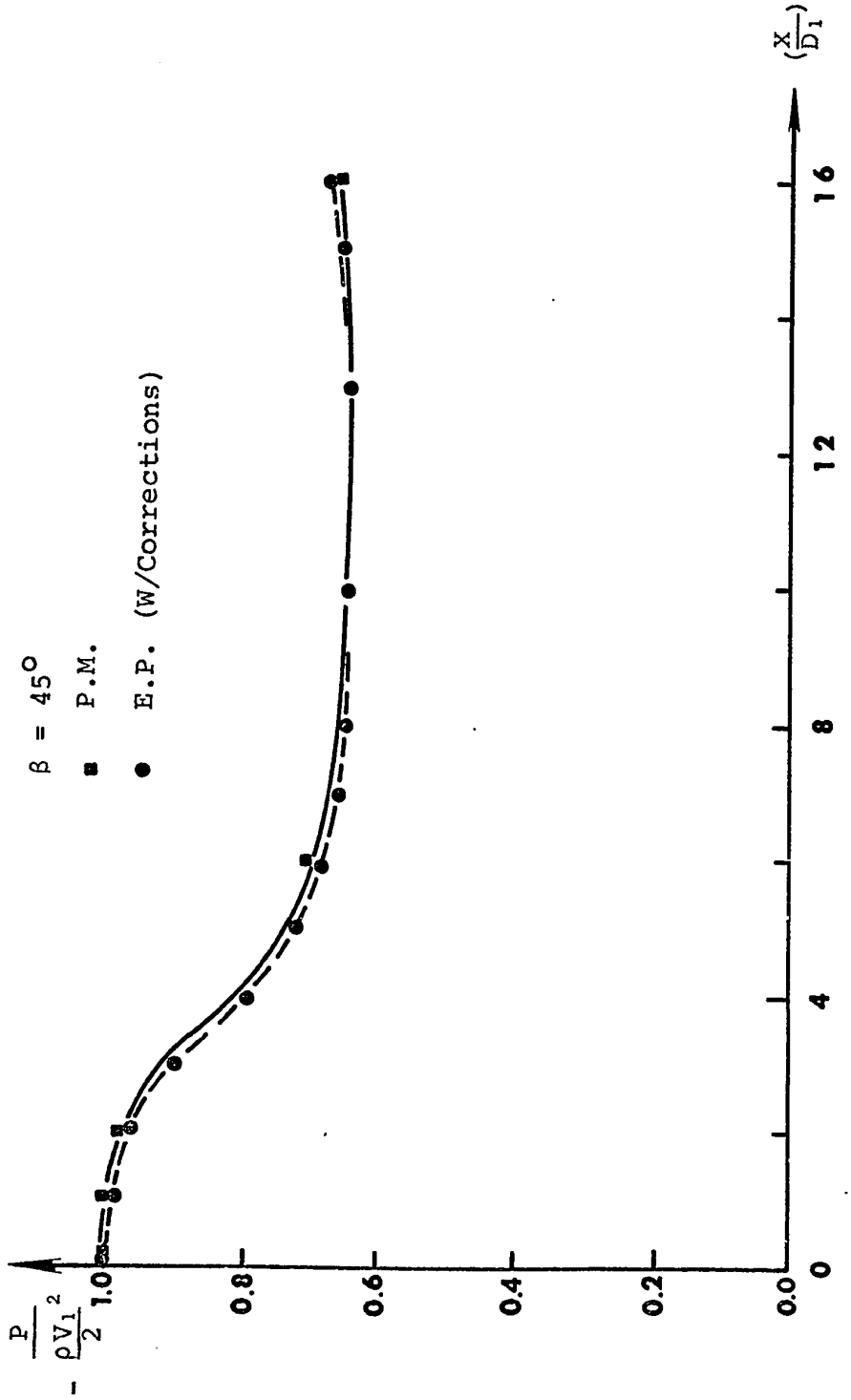

FIG. 26 The Center-Line Value of Pressure, for β = 45°

APPENDIX I

DERIVATION OF CORRECTION FACTOR (ρ_x/ρ_y) FOR CONDUCTING PAPER

APPENDIX I

DERIVATION OF CORRECTION FACTOR (ρ_x/ρ_y) FOR CONDUCTING PAPER

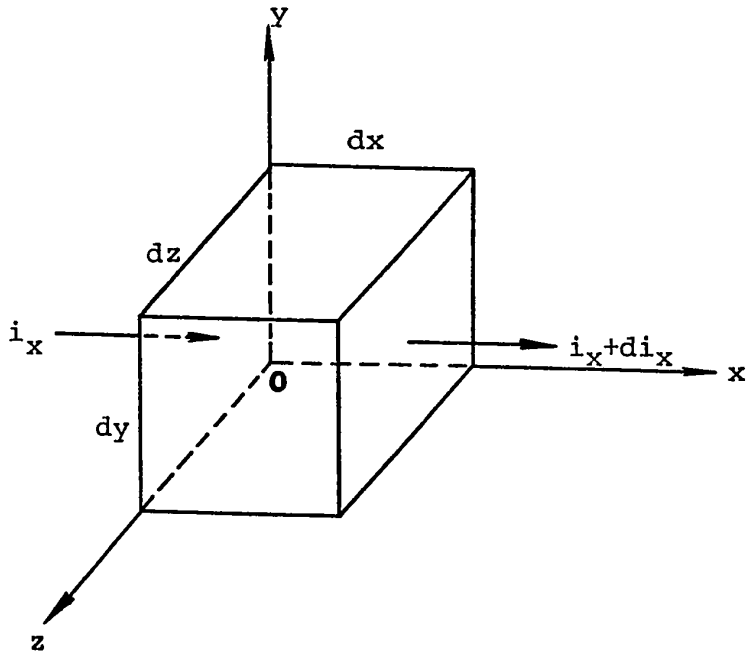

FIG. A.1. The Element of Current Density

As in Fig. A-1, consider i_x, i_y and i_z as the components of current density in directions OX, OY and OZ of the element dxdydz and then

current density on face dydz (at x = 0) = i_x

current entering this face = $i_x dydz$

current leaving the opposite face (at x = dx) =

$$= (i_x + \frac{\partial i_x}{\partial x} dx)$$

Similarly for the other faces, since the total current entering should be equal to the total current leaving, thus

$$i_x dydz + i_y dxdz + i_z dxdy = (i_x + \frac{\partial i_x}{\partial x} dx) dydz \; (i_y + \frac{\partial i_y}{\partial y} dy) dxdz + + (i_z + \frac{\partial i_z}{\partial z}) dxdy$$

Hence

$$\frac{\partial i_x}{\partial x} + \frac{\partial i_y}{\partial y} + \frac{\partial i_z}{\partial z} = 0 \qquad \text{(A.1)}$$

In this case of conducting paper dz is small and constant, therefore

$$\frac{\partial i_z}{\partial z} = 0$$

Thus eqn. (A.1) becomes

$$\frac{\partial i_x}{\partial x} + \frac{\partial i_y}{\partial y} = 0 \qquad \text{(A.2)}$$

Again, by Ohm's Law, current density = $(i_x/a) = (V/\rho_x x)$, where ρ_x is the resistivity in ohms per unit area in the x direction. Thus $i_x = - \frac{\partial V}{\partial x} \frac{1}{\rho_x}$, the voltage gradient decreasing in the direction of the current flow.

Similarly,

$$i_y = - \frac{\partial V}{\partial y} \frac{1}{\rho_y}$$

Substituting in eqn. (A.2) becomes

$$- \frac{1}{\rho_x} \frac{\partial^2 V}{\partial x^2} - \frac{1}{\rho_y} \frac{\partial^2 V}{\partial y^2} = 0 \qquad \text{(A.3)}$$

If $\rho_x = \rho_y$, then eqn. (A.3) becomes

$$\frac{\partial^2 V}{\partial x^2} + \frac{\partial^2 V}{\partial y^2} = 0 \qquad (A.4)$$

However, since $\rho_x \neq \rho_y$, in the case of the conducting paper, it is necessary to introduce a correction factor.

Assuming that the x ordinates are altered to some value $u = f(x)$ in order to compensate for the inequality between ρ_x and ρ_y, eqn. (A.2) becomes

$$\frac{\partial i_u}{\partial x}\frac{\partial x}{\partial u} + \frac{\partial i_y}{\partial y} = 0 \qquad (A.5)$$

And also,

$$i_u = -\frac{1}{\rho_u}\frac{\partial V}{\partial u} = -\frac{1}{\rho_u}\frac{\partial V}{\rho x}\frac{\partial x}{\partial u}$$

as before

$$i_y = -\frac{\partial V}{\partial y}\frac{1}{\rho_y}$$

Substituting eqn. (A.5) becomes

$$\frac{1}{\rho_x}\left(\frac{\partial x}{\partial u}\right)^2\frac{\partial^2 V}{\partial x^2} + \frac{1}{\rho_x}\frac{\partial x}{\partial u}\frac{\partial V}{\partial x}\frac{\partial}{\partial x}\left(\frac{\partial x}{\partial u}\right) + \frac{1}{\rho_y}\frac{\partial^2 V}{\partial y^2} = 0 \qquad (A.6)$$

To make this equation of the same form as eqn. (A.4), first, the term

$$\frac{1}{\rho_x}\frac{\partial x}{\partial u}\frac{\partial V}{\partial x}\frac{\partial}{\partial x}\left(\frac{\partial x}{\partial u}\right)$$

must be equal to zero. Since $\partial V/\partial x$ is not zero, $(\partial/\partial x)(\partial x/\partial u)$ must be made zero, in which case $\partial x/\partial u$ must be a constant, which implies that u is a linear function of x.

Secondly, from eqns. (A.4) and (A.6), $(1/\rho_x)(\partial x/\partial u)^2$ must be made equal to $(1/\rho_y)$, that is

$$\partial x/\partial u = (\rho_x/\rho_y)^{\frac{1}{2}}$$

which is constant. Both of these conditions are satisfied simultaneously by putting

$$u = x(\rho_y/\rho_x)^{\frac{1}{2}}$$

Hence, if $\rho_x \neq \rho_y$, all dimensions in the x direction must be multiplied by $(\rho_x/\rho_y)^{\frac{1}{2}}$. Alternatively, all dimensions in the y direction must be multiplied by $(\rho_y/\rho_x)^{\frac{1}{2}}$.

When these conditions are satisfied

$$\frac{\partial^2 V}{\partial x^2} + \frac{\partial^2 V}{\partial y^2} = 0$$

APPENDIX II

EVALUATION OF THE CENTER-LINE VALUES OF VELOCITY AND PRESSURE IN AN ABRUPT ENLARGEMENT

APPENDIX II

EVALUATION OF THE CENTER-LINE VALUES OF VELOCITY AND PRESSURE IN AN ABRUPT ENLARGEMENT

```
      PROGRAM ISOFLOW (INPUT,OUTPUT,TAPE61=OUTPUT,TAPE60=INPUT)
      DIMENSION ALF(20), AA(20)

1000  FORMAT (8F10.0)
1010  FORMAT (1HO,9E14.6)

      READ (60,1000) (ALF(I), AA(I), I=1,14)
      DO 1020 J=1,14
      SA=AA(J)*(AA(J)
      V=O
      DO 1020 K=1,11
      VV=V*V
      P=ALF(J)-VV*(1.-SA)
      WRITE (61,1010)ALF(J),AA(J), V,P
      V=V+.1

1020  CONTINUE

      END
```

DATA

0.	1.	.1	1.	.2	1.	3.	1.
.4	1.	.5	1.	.6	1.	.7	1.
.75	.74	.77	.65	.80	.35	.82	.29
.90	.33	1.	.33				

MATHEMATICAL SYMBOLS	FORTRAN CODE
α	ALF
$\frac{A_1}{A}$	AA
$\overline{V}$	V
ΔP	P

APPENDIX III

EVALUATION OF $\Delta h_{1.2}$ IN AN ABRUPT ENLARGEMENT ($\beta = 90^{o}$)

APPENDIX III

EVALUATION OF $\Delta h_{1\text{-}2}$ IN AN ABRUPT ENLARGEMENT ($\beta = 90^{o}$)

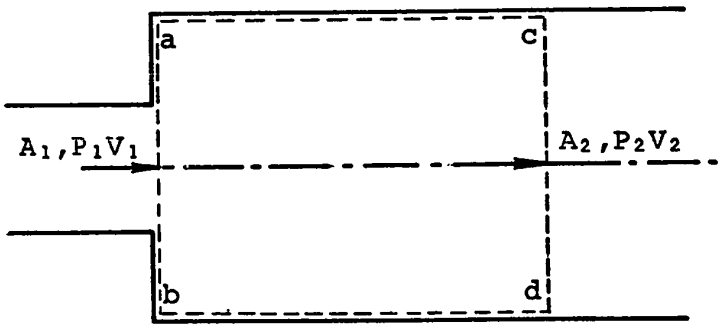

FIG. A.2 The Fluid Flow Through an Abrupt Enlargement

As shown in Figure A.2, consider the control surface of a b c d (*), drawn to enclose the zone of momentum change, then the flowrate Q through the volume is

$$Q = A_1V_1 = A_2V_2 \qquad (A.7)$$

While the rate of change of momentum is given by

$$\frac{d}{dt}(MV) = \dot{M}V_2 - \dot{M}V_1$$

$$= \frac{Q\rho g}{g}(V_2 - V_1)$$

$$= \frac{A_1V_1\rho g}{g}(V_2 - V_1) \qquad (A.8)$$

Since the forces producing these changes of momentum act on the surface of a b and c d, may be assumed to result from hydrostatic pressure distribution over the areas and can be evaluated as

$$\Sigma F_x = P_1 A_2 - P_2 A_2 = A_2(P_1 - P_2) = \frac{d}{dt}(MV)_x \qquad (A.9)$$

From eqns. (A.8) and (A.9)

$$\frac{A_1 V_1 \rho g}{g}(V_2 - V_1) = A_2(P_1 - P_2)$$

or

$$\frac{V_2(V_2 - V_1)}{g} = \frac{P_1 - P_2}{\rho g} \qquad (A.10)$$

Substituting eqns. (A.7) and (A.10) in Euler's equation, or Bernoulli's theory, as derived before in Chapter II, we have

$$\Delta h_{12} = \frac{P_1 - P_2}{\rho g} - \frac{V_2^2 - V_1^2}{2g} = \frac{V_2(V_2 - V_1)}{g} - \frac{V_2^2 - V_1^2}{2g} = \frac{V_1^2}{2g}\left[1 - \frac{A_1}{A_2}\right]^2 \qquad (A.11)$$

(*) This is a good assumption for the surface along the cross-section of c d. For cross-sectional surface a b, it is an approximation because of the dynamics of the eddies in the "dead zone". Accordingly, the result of the analysis will be approximate and the required experimental veri-

fication shows that in

$$\Delta h_{1,2} = K\frac{(V_1 - V_2)^2}{2g}$$

in which $K \simeq 1$ is confirmed within a few percentage, making it quite adequate for engineering applications.[16]

APPENDIX IV

EVALUATION OF $\Delta h_{1\text{-}2}$ IN A GRADUAL ENLARGEMENT

APPENDIX IV

EVALUATION OF $\Delta h_{1\text{-}2}$ IN A GRADUAL ENLARGEMENT

The head loss in a fluid flowing duct due to gradual enlargment will be dependent upon the shape of the enlargement.[16] Tests have been carried out on the losses in conical enlargements, and the results are expressed by the equation

$$\Delta h_{12} = K \frac{(V_1 - V_2)^2}{2g} \qquad (A.12)$$

in which K is primarily dependent upon the cone angle but also a function of the area ratio, as shown in Fig. A.3.

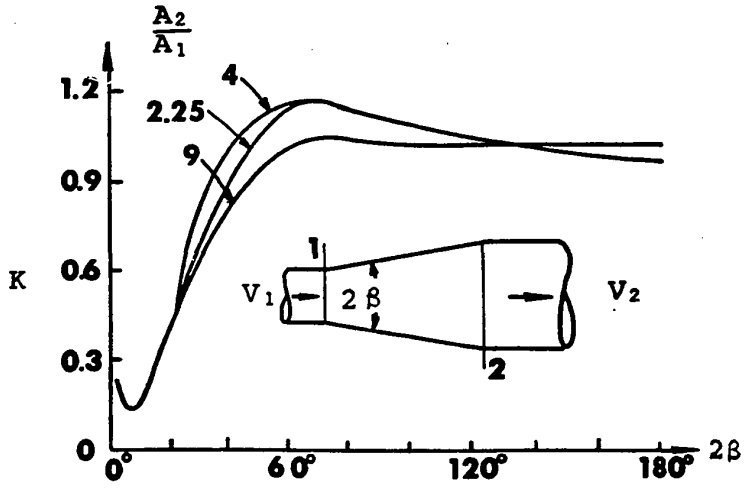

FIG. A.3 Head Loss Coefficients for Conical Enlargements

Since the prototype we used here is a cone of $2\beta = 30^{\circ}$ and $2\beta = 90^{\circ}$, and the ratio of $A_2/A_1 = 4$, the value of K is about 0.8 and 1.0, respectively, as shown in Fig. A.3.